THE ASTROPHYSICAL JOURNAL, 462:241–254, 1996 May 1

THE GIANT BRANCH OF ω CENTAURI. V. THE CALCIUM ABUNDANCE DISTRIBUTION

JOHN E. NORRIS,[1] K. C. FREEMAN,[2] AND K. J. MIGHELL[3]
Mount Stromlo and Siding Spring Observatories, The Australian National University,
Private Bag, Weston Creek P.O., A.C.T. 2611, Australia
Received 1995 August 21; accepted 1995 November 3

ABSTRACT

We present an unbiased catalog of calcium abundances for 517 red giants brighter that $M_V \sim -1$ in the chemically inhomogeneous globular cluster ω Centauri. The basic features of the abundance distribution are as follows: (1) few, if any, stars exist on the giant branch of ω Cen with [Ca/H] less than −1.6; (2) there is a well-defined peak in the distribution at [Ca/H] = −1.4, with a long tail stretching up to ∼[Ca/H] ∼ −0.3; and (3) the distribution is bimodal with a second smaller peak in the distribution at [Ca/H] = −0.9.

The distribution may be well fitted by two components each having a simple closed box abundance distribution and for which the ratio of more metal rich to more metal poor is ∼0.2. We argue that the present data, taken together with the abundance patterns of the *s*-process elements in this cluster reported by in 1994 by Vanture, Wallerstein, & Brown and in 1995 by Norris & Da Costa, are most convincingly described in terms of the two components representing successive epochs of star formation in the cluster, rather than of their being two independent merging fragments. Examination of the radial distribution of [Ca/H] suggests that there is an abundance gradient in the cluster, consistent with its having been formed in a dissipative manner.

The picture emerges of ω Cen having evolved within the Searle-Zinn paradigm of Galactic globular cluster formation, from a gaseous protocloud of mass perhaps as large as $\sim 10^8\ M_\odot$ and initial abundance [Ca/H] ∼ −1.5 on a timescale ∼1 Gyr, well away from the central region of the forming Galaxy and later coming into dynamical equilibrium with it.

Subject headings: globular clusters: individual (ω Centauri) — stars: abundances — stars: late-type — stars: Population II

1. INTRODUCTION

The chemical inhomogeneity of ω Centauri, the most massive Galactic globular cluster, is now well established and results from both enrichment during the formation of the cluster and later evolutionary mixing effects. Since the first reports of the abundance variations by Freeman & Rodgers (1975) and Norris & Bessell (1975), it has become evident that the iron-to-hydrogen ratio extends from 1/60 solar up to perhaps one-third solar and that large ranges (not all in lockstep with those of iron) exist for all other elements studied to date. We refer the reader to the reviews of Kraft (1979, 1994), Freeman & Norris (1981), Smith (1987), and Suntzeff (1993) concerning the historical development of the subject and to the work of Brown & Wallerstein (1993), Vanture, Wallerstein, & Brown (1994), Norris & Da Costa (1995), and references therein for recent advances.

However, in spite of the two decades since the demonstration of this inhomogeneity, most, if not all, of the investigations of the chemical abundance patterns of this system are based on inherently biased samples, and the form of the abundance distribution and its implications concerning cluster formation have not been well determined. Most investigations relevant to this question suffer from one or another of the disadvantages of relatively small sample size, relatively large abundance errors, and field contamination. We identify four works as currently having most relevance to the nature of the abundance distribution. They are (1) the investigation of some 55 RR Lyrae variables by Butler, Dickens, & Epps (1978); (2) the histogram of [Ca/H] presented by Norris (1980) for 100 red giants; (3) the histograms of the abundance-related parameter $R(V-K)$ of Persson et al. (1980) for biased and unbiased samples containing 79 and 46 red giants, respectively; and (4) the $B-V$ histogram of Da Costa & Villumsen (1981) for some ∼200 subgiants. The general features of the abundance distributions presented in these works are as follows: (1) few if any stars with [Fe/H] < −1.8, (2) a strong peak in the distribution at [Fe/H] ∼ −1.6, (3) a long tail to higher abundance up to perhaps [Fe/H] = −0.5, and (4) a possible bimodality with the second smaller peak at [Fe/H] ∼ −1.2.

The purpose of the present paper is to present observations of an unbiased sample of some 500 red giants in the cluster to constrain more strongly the form of the abundance distribution. In §§ 2 and 3 we define the sample and present medium-resolution spectra taken in the region of the Ca II H and K lines and of the infrared calcium triplet. Calcium abundances are determined and compared with the results of other investigations in § 4. In §§ 5 and 6 we examine the form of the distribution, which is bimodal, together with the question of a radial [Ca/H] gradient. Finally, in § 7 we discuss the ramifications of these results for the formation and evolution of the cluster.

[1] E-mail: jen@mso.anu.edu.au.
[2] E-mail: kcf@mso.anu.edu.au.
[3] Present address: Department of Astronomy, Columbia University, 538 West 120th Street, New York, NY 10027.
E-mail: mighell@susanna.phys.columbia.edu.

TABLE 1

Ca II Line Strength Measurements and Abundances for ω Centauri Giants

Star	V[a]	Ref	r	A(Ca)	W	n[b]	[Ca/H]	Star	V[a]	Ref	r	A(Ca)	W	n[b]	[Ca/H]	Star	V[a]	Ref	r	A(Ca)	W	n[b]	[Ca/H]
(1)	(2)	(3)	(4)	(5)	(6)	(7)	(8)	(1)	(2)	(3)	(4)	(5)	(6)	(7)	(8)	(1)	(2)	(3)	(4)	(5)	(6)	(7)	(8)
35	11.49	2	3.6	.....	4.93	001	−1.41	119	12.21	2	5.0	.....	5.07	010	−1.17	207	12.18	3	19.5	.....	5.41	010	−1.05
39	11.80	2	3.5	.....	6.11	010	−0.87	120	11.97	3	7.1	.....	4.96	001	−1.28	208	12.30	3	6.9	.....	5.40	010	−1.02
40	11.37	1	9.4	.....	5.22	010	−1.33	122	12.01	2	3.9	.....	4.70	010	−1.37	209	12.18	3	11.6	.....	4.48	011	−1.41
41	11.64	2	2.6	.....	4.80	010	−1.42	123	12.05	2	2.5	.....	4.57	010	−1.41	210	12.49	2	3.5	.....	4.35	012	−1.38
42	11.64	3	4.4	.....	5.30	030	−1.23	124	11.83	1	8.9	.....	4.91	010	−1.33	211	12.27	3	8.0	.....	7.02	010	−0.38
43	11.62	1	18.5	.....	5.35	0**	−1.22	125	11.99	3	7.0	.....	4.63	010	−1.40	212	12.20	3	14.6	.....	4.66	011	−1.34
44	11.63	3	5.5	.....	5.16	010	−1.29	127	12.04	2	3.1	.....	4.57	010	−1.41	213	12.22	1	12.9	.....	4.12	011	−1.54
45	11.88	2	4.0	.....	4.91	010	−1.32	130	12.07	2	2.8	.....	4.98	010	−1.25	215	12.44	2	3.4	.....	4.74	011	−1.24
46	11.54	1	8.0	.....	5.10	021	−1.33	131	12.07	3	5.2	.....	4.82	010	−1.31	217	12.21	3	17.5	.....	4.60	021	−1.36
48	11.51	1	6.3	.....	4.89	020	−1.42	132	12.05	3	5.9	.....	5.39	010	−1.09	218	12.21	3	17.5	.....	4.91	010	−1.24
49	11.58	1	5.6	.....	5.08	010	−1.33	133	11.99	3	8.7	.....	4.63	010	−1.40	219	12.20	1	15.3	.....	6.43	013	−0.64
51	11.69	3	4.9	.....	4.93	020	−1.36	134	12.07	3	5.9	.....	4.92	010	−1.27	220	12.34	3	6.3	.....	5.67	010	−0.90
52	11.67	3	5.6	.....	4.43	010	−1.56	135	12.06	3	6.2	.....	5.90	010	−0.89	221	12.33	3	6.6	.....	4.33	001	−1.43
53	11.58	1	16.6	.....	5.16	030	−1.30	138	12.11	3	4.9	.....	5.57	020	−1.00	224	12.24	2	5.3	.....	4.52	010	−1.38
54	11.71	2	4.7	.....	4.95	010	−1.35	139	11.98	3	10.0	.....	5.51	010	−1.06	229	12.34	3	7.5	.....	5.33	011	−1.04
56	11.68	1	18.6	.....	5.45	010	−1.16	141	12.09	3	6.1	.....	4.22	010	−1.53	231	12.37	3	6.4	.....	6.52	011	−0.56
58	11.67	1	8.7	.....	4.73	011	−1.44	144	12.38	2	4.5	.....	5.17	010	−1.09	232	12.25	3	11.5	0.421	4.69	211	−1.29
59	11.71	3	5.6	.....	5.12	010	−1.28	146	11.98	3	13.4	.....	4.90	010	−1.30	233	12.28	3	10.1	0.380	4.46	111	−1.40
61	11.60	1	9.1	.....	4.84	010	−1.42	147	12.11	3	6.5	.....	4.71	010	−1.34	234	12.25	1	12.7	0.370	4.09	111	−1.52
62	11.50	1	5.0	.....	5.33	010	−1.25	148	12.28	2	3.3	.....	5.95	020	−0.81	235	12.38	3	6.3	0.428	4.85	211	−1.20
63	11.72	2	3.0	.....	5.17	020	−1.26	150	12.00	1	14.6	.....	6.25	012	−0.76	236	12.37	2	4.3	.....	5.75	020	−0.86
64	11.73	2	3.2	.....	4.98	020	−1.33	151	12.16	3	5.1	.....	5.89	020	−0.86	237	12.59	2	3.5	.....	5.94	010	−0.73
65	11.61	1	6.7	.....	4.73	011	−1.46	152	12.18	3	4.8	.....	4.16	020	−1.53	238	12.58	2	3.7	0.381	4.39	211	−1.34
66	11.53	1	12.5	.....	5.11	010	−1.33	155	12.00	1	16.4	.....	5.19	010	−1.18	239	12.41	3	5.7	.....	5.72	010	−0.87
67	11.64	1	6.6	.....	4.83	010	−1.41	157	12.22	2	4.9	.....	5.48	040	−1.01	240	12.27	3	16.4	0.481	5.91	111	−0.87
69	11.72	3	7.5	.....	4.89	010	−1.37	158	12.08	3	9.3	.....	6.16	010	−0.78	243	12.36	3	8.0	0.492	5.83	311	−0.85
70	11.61	1	19.3	.....	5.51	010	CH	159	12.04	1	15.6	.....	4.69	010	−1.37	244	12.40	2	4.8	0.428	5.17	311	−1.11
71	11.82	3	4.5	.....	5.21	010	−1.22	160	12.10	3	8.8	.....	5.79	010	−0.92	245	12.28	3	13.7	0.494	5.64	211	−0.91
73	11.70	1	9.1	.....	4.83	010	−1.40	161	11.97	1	11.3	.....	4.89	010	−1.31	246	12.44	1	7.1	0.410	4.61	311	−1.28
74	11.78	1	8.8	.....	4.64	020	−1.45	162	12.14	1	16.3	.....	5.81	010	−0.90	247	12.59	2	5.1	0.397	4.40	211	−1.31
75	11.80	3	5.9	.....	4.54	010	−1.48	163	12.19	3	5.6	.....	4.64	030	−1.35	248	12.43	3	5.9	0.512	6.35	111	−0.66
76	11.79	3	6.6	.....	5.24	020	−1.22	166	12.24	3	4.3	.....	6.55	020	−0.58	249	12.46	3	4.9	0.424	4.87	211	−1.18
77	11.84	3	5.4	.....	4.74	010	−1.40	167	12.16	2	4.5	.....	4.56	030	−1.39	251	12.34	3	9.6	0.442	4.87	211	−1.18
78	11.83	2	2.6	.....	4.62	010	−1.45	168	12.46	2	3.5	.....	4.98	020	−1.15	252	12.30	3	15.2	0.388	4.38	*12	−1.41
79	11.84	2	4.7	.....	5.13	011	−1.25	169	12.21	2	4.7	.....	5.00	020	−1.20	253	12.34	1	17.0	0.486	5.50	512	−0.95
80	11.69	2	2.5	.....	4.11	010	−1.68	170	12.10	3	9.8	.....	4.53	010	−1.41	254	12.58	2	5.3	0.390	4.53	211	−1.29
81	11.84	3	6.3	.....	5.40	010	−1.14	171	12.07	1	11.1	.....	5.70	010	−0.96	255	12.38	3	8.2	0.392	4.64	311	−1.31
82	11.71	3	22.4	.....	4.65	010	−1.46	172	12.10	3	9.9	.....	5.06	010	−1.21	256	12.37	3	8.9	0.399	4.57	111	−1.32
84	11.87	1	6.4	.....	6.18	020	−0.82	174	12.16	2	4.8	.....	5.54	020	−1.00	258	12.40	3	7.7	0.402	4.45	211	−1.34
85	11.84	1	5.9	.....	5.81	010	−0.98	175	12.26	3	4.3	.....	5.74	010	−0.90	259	12.51	3	4.1	.....	4.84	011	−1.19
86	11.87	3	5.8	.....	5.06	001	−1.26	177	12.20	3	6.4	.....	5.26	010	−1.10	260	12.35	3	9.9	0.440	4.69	111	−1.23
88	11.85	2	2.7	.....	4.80	020	−1.37	178	12.20	3	6.6	.....	5.22	010	−1.12	261	12.42	3	7.5	0.420	4.72	211	−1.24
89	11.82	3	8.2	.....	5.39	010	−1.15	179	12.21	3	6.3	.....	6.73	010	−0.52	262	12.48	3	5.4	0.386	4.67	111	−1.29
90	11.66	1	18.5	.....	5.54	010	−1.13	180	12.08	3	12.5	.....	4.43	010	−1.46	263	12.52	3	4.1	.....	5.68	010	−0.85
91	11.84	1	14.4	.....	4.75	010	−1.39	181	12.13	3	9.6	.....	4.70	010	−1.34	265	12.51	3	4.9	.....	4.45	011	−1.34
92	11.93	2	3.8	.....	5.58	020	−1.05	182	12.24	3	5.9	.....	5.64	010	−0.94	266	12.48	3	5.7	0.381	4.15	111	−1.43
94	11.80	1	9.5	.....	4.73	010	−1.41	183	12.12	3	10.1	.....	4.72	010	−1.33	267	12.52	3	4.5	.....	5.73	010	−0.83
95	11.77	1	9.3	.....	5.33	010	−1.19	184	12.10	3	10.5	.....	5.31	010	−1.11	268	12.50	3	5.7	.....	4.53	010	−1.31
96	11.78	1	14.7	.....	5.01	010	−1.31	185	12.21	3	6.8	.....	4.69	010	−1.32	269	12.35	1	11.9	0.408	4.56	211	−1.31
97	11.91	2	3.6	.....	4.61	010	−1.43	188	12.33	2	4.1	.....	5.30	020	−1.05	270	12.42	1	9.7	0.487	5.89	112	−0.82
99	12.72	2	3.6	.....	5.08	040	−1.04	191	12.31	3	4.4	.....	5.22	010	−1.09	271	12.36	3	11.0	0.395	4.63	111	−1.32
100	11.91	2	4.3	.....	5.77	030	−0.98	192	12.22	3	7.5	.....	5.33	010	−1.07	272	12.38	1	17.4	0.433	4.86	111	−1.19
101	11.99	2	2.8	.....	4.41	001	−1.48	193	12.18	3	9.2	.....	4.46	010	−1.42	275	12.45	3	7.9	0.381	4.12	111	−1.45
102	11.68	1	15.3	.....	4.76	020	−1.43	194	12.13	3	16.2	.....	5.11	010	−1.18	276	12.55	3	4.5	.....	6.64	011	−0.46
104	11.95	2	4.0	.....	4.72	020	−1.38	195	12.29	3	5.2	.....	5.26	010	−1.08	277	12.51	3	5.6	0.378	4.43	111	−1.36
105	11.94	3	6.0	.....	5.24	010	−1.18	197	12.33	3	4.0	.....	4.24	010	−1.47	278	12.49	3	6.5	0.422	4.49	111	−1.28
106	11.96	2	3.1	.....	4.72	010	−1.37	198	12.40	2	4.1	.....	4.52	010	−1.34	279	12.32	1	18.0	0.310	4.37	211	CH
107	11.93	2	2.8	.....	5.67	010	−1.01	199	12.14	3	14.6	.....	4.92	010	−1.25	280	12.37	3	21.9	0.414	4.91	311	−1.21
108	11.93	2	4.9	.....	5.86	010	−0.94	200	12.30	3	5.5	.....	4.17	014	−1.50	281	12.51	3	6.2	.....	4.94	030	−1.15
109	11.81	3	14.1	.....	4.79	010	−1.38	201	12.17	2	3.9	.....	6.13	014	−0.77	282	12.43	3	8.9	0.388	4.35	111	−1.38
110	11.78	1	6.6	.....	5.85	010	−0.98	202	12.37	2	3.9	.....	5.09	010	−1.13	285	12.61	2	3.7	.....	4.26	010	−1.39
111	12.25	2	5.9	.....	4.40	010	−1.42	203	12.45	2	4.5	.....	4.37	010	−1.39	286	12.57	3	4.4	.....	6.11	021	−0.67
115	11.92	3	7.5	.....	4.75	010	−1.37	205	12.26	3	7.4	.....	4.50	010	−1.38	287	12.41	1	13.7	0.446	5.49	311	−1.00
117	12.01	2	2.8	.....	5.84	010	−0.92	206	12.30	3	6.5	.....	4.97	011	−1.19	288	12.48	3	7.9	0.375	4.28	111	−1.41

2. THE UNBIASED SAMPLE

We sought to obtain spectra for as large as possible a sample of ω Cen red giants brighter than $V \sim 13$ ($M_V \sim -0.9$) with the explicit requirement that no bias be introduced into the selection procedure with respect to color or the spectroscopic properties of the sample.

The only objects deliberately excluded from the sample were those that, based on the work of Woolley et al. (1966), are probable nonmembers of the cluster on proper motion and color-magnitude diagram criteria (their class "f"), that are radial velocity nonmembers based on Cannon & Stobie (1973a) and the present work, or that presented observational difficulties because of close companions or problems of identification.[4]

The final sample of 521 cluster members is presented in Table 1. The objects come from several sources. Most were

[4] Our radial velocity measurements show that ROA 129, 137, 153, 154, 165, 189, 225, 388, 411, 413, 482, 487, 491, and 506 are not cluster members. The CH star ROA 55 was observed in the infrared during this program but is not included in Table 1 because of severe line blending.

TABLE 1—*Continued*

Star	V[a]	Ref	r	A(Ca)	W	n[b]	[Ca/H]	Star	V[a]	Ref	r	A(Ca)	W	n[b]	[Ca/H]	Star	V[a]	Ref	r	A(Ca)	W	n[b]	[Ca/H]
(1)	(2)	(3)	(4)	(5)	(6)	(7)	(8)	(1)	(2)	(3)	(4)	(5)	(6)	(7)	(8)	(1)	(2)	(3)	(4)	(5)	(6)	(7)	(8)
289	12.44	1	8.4	0.391	4.65	111	−1.30	373	12.71	3	7.3	.....	3.52	001	−1.65	451	12.89	3	7.4	.....	6.24	001	−0.54
290	12.40	3	11.2	.....	4.18	011	−1.47	374	12.78	3	4.6	.....	3.47	001	−1.65	452	12.99	3	3.8	.....	4.17	001	−1.33
292	12.56	3	5.3	0.354	4.23	111	−1.43	375	12.72	3	7.2	0.351	3.86	101	−1.48	453	12.99	3	3.7	.....	5.60	001	−0.76
293	12.58	2	4.5	0.432	5.05	121	−1.09	376	12.76	3	5.8	0.471	5.27	101	−0.91	454	12.99	3	3.8	.....	3.65	001	−1.53
294	12.56	3	5.3	.....	4.87	020	−1.16	378	12.63	3	12.5	0.439	4.75	101	−1.12	455	12.95	3	5.4	.....	4.73	001	−1.12
296	12.43	3	10.4	0.378	4.43	*31	−1.38	379	12.62	1	11.3	0.387	4.44	101	−1.31	456	12.94	3	5.8	.....	4.05	001	−1.39
297	12.44	1	15.4	0.408	4.84	121	−1.22	380	12.68	1	9.1	.....	4.49	001	−1.28	457	12.86	3	8.9	0.323	.....	100	−1.54
299	12.57	3	5.5	.....	3.91	001	−1.53	381	12.63	3	17.8	0.403	4.77	101	−1.20	458	12.94	3	6.2	0.403	.....	100	−1.14
300	12.71	2	3.8	.....	7.52	021	−0.06	382	12.78	3	5.7	0.392	.....	100	−1.24	461	12.85	3	9.4	.....	4.66	001	−1.17
301	12.53	2	4.4	0.458	5.33	111	−0.99	383	12.81	3	4.7	.....	4.46	001	−1.26	462	12.76	1	8.6	.....	3.64	001	−1.59
302	12.54	3	6.7	.....	4.17	010	−1.44	385	12.76	3	6.7	0.352	4.41	101	−1.36	463	12.81	3	10.8	.....	6.75	001	−0.35
303	12.52	3	7.7	0.386	4.18	121	−1.40	387	12.65	3	12.9	0.341	.....	100	−1.51	464	12.85	1	15.9	0.382	.....	100	−1.27
304	12.61	3	4.5	.....	4.59	010	−1.26	389	12.65	3	15.8	0.405	.....	100	−1.21	465	12.81	3	11.5	.....	5.58	002	−0.82
305	12.58	1	8.1	0.362	4.23	111	−1.41	390	12.79	3	6.2	.....	4.18	001	−1.37	467	12.85	2	4.7	.....	4.02	001	−1.42
307	12.49	3	9.5	0.387	4.16	111	−1.41	391	12.80	2	4.5	0.343	.....	100	−1.46	468	12.98	3	5.1	.....	3.55	001	−1.57
308	12.65	2	4.4	0.388	4.28	111	−1.34	392	12.92	2	3.4	.....	4.38	001	−1.26	469	12.93	2	4.7	.....	4.52	001	−1.20
309	12.76	2	4.0	.....	4.24	020	−1.36	393	12.84	3	4.3	.....	4.22	001	−1.35	470	12.82	1	11.7	.....	4.20	001	−1.36
311	12.64	3	4.5	.....	4.42	010	−1.32	394	12.66	1	19.5	0.479	.....	100	−0.85	472	12.83	3	10.8	.....	5.82	001	−0.72
312	12.44	1	15.9	0.414	4.74	211	−1.24	395	12.67	3	10.6	.....	4.68	001	−1.21	473	12.88	1	11.4	.....	4.15	001	−1.36
313	12.55	1	7.6	.....	5.31	010	−0.99	396	12.66	3	18.5	0.439	.....	100	−1.04	474	12.81	1	13.1	0.324	.....	100	−1.55
315	12.63	3	5.1	0.413	4.64	101	−1.20	397	12.82	3	5.3	.....	3.89	001	−1.48	476	12.79	1	18.7	0.341	.....	100	−1.48
316	12.47	3	16.5	0.535	6.41	101	−0.60	398	12.80	1	7.7	.....	4.45	001	−1.27	477	12.97	3	5.6	.....	3.83	001	−1.46
318	12.67	3	4.1	.....	4.15	001	−1.41	400	12.67	3	14.3	0.414	.....	100	−1.16	479	12.99	3	5.1	.....	4.35	001	−1.26
319	12.50	3	10.3	0.397	4.64	101	−1.28	402	12.68	1	13.7	0.344	.....	100	−1.49	480	12.98	3	5.6	0.547	.....	100	−0.44
320	12.75	1	6.9	0.472	5.82	101	−0.80	403	12.68	3	21.9	.....	4.15	001	−1.41	481	12.88	1	17.5	0.328	.....	100	−1.51
321	12.66	3	5.2	0.544	6.27	101	−0.56	404	12.82	3	6.1	.....	4.46	001	−1.26	483	12.82	1	15.7	.....	4.07	001	−1.41
322	12.52	3	10.3	.....	5.51	001	−0.92	405	12.85	3	5.0	.....	4.72	001	−1.15	484	12.83	3	21.7	0.361	.....	100	−1.37
324	12.59	3	8.2	.....	6.98	001	−0.32	406	12.88	3	4.1	.....	5.26	001	−0.93	485	12.98	3	5.7	.....	4.21	001	−1.31
325	12.51	3	13.8	0.349	4.20	101	−1.47	407	12.73	3	9.5	.....	5.27	001	−0.96	486	13.02	3	4.5	.....	4.58	001	−1.16
326	12.65	3	6.2	.....	4.52	001	−1.28	408	12.69	3	12.1	0.360	.....	100	−1.41	489	12.94	3	7.4	0.391	.....	100	−1.20
327	12.67	3	5.5	0.418	5.25	101	−1.06	410	12.86	2	4.0	.....	4.10	001	−1.39	490	12.93	3	7.7	.....	4.02	001	−1.40
328	12.71	2	3.8	.....	4.24	001	−1.37	412	12.80	3	7.0	.....	5.25	001	−0.95	493	12.85	3	14.2	.....	3.51	001	−1.62
329	12.64	2	4.0	0.464	5.27	101	−0.96	414	12.86	3	5.5	.....	5.41	001	−0.87	494	13.04	3	4.3	.....	3.77	001	−1.47
330	12.65	2	3.9	0.385	5.32	101	−1.13	415	12.66	1	9.7	.....	4.25	001	−1.38	496	12.87	3	10.5	.....	4.11	001	−1.38
332	12.57	3	9.4	0.468	6.47	101	−0.73	416	12.87	3	5.3	.....	4.51	001	−1.22	498	13.02	3	5.3	.....	4.85	001	−1.05
334	12.53	3	10.6	0.382	4.23	101	−1.38	418	12.70	1	11.7	0.344	.....	100	−1.48	499	12.96	3	7.4	.....	4.06	001	−1.38
336	12.91	2	3.5	.....	6.72	001	−0.33	419	12.97	2	3.9	0.482	.....	100	−0.76	500	13.06	3	4.0	.....	7.53	001	0.03
337	12.63	3	7.2	0.378	4.22	101	−1.37	420	12.92	3	4.1	.....	3.94	001	−1.43	501	12.93	3	9.1	.....	3.89	001	−1.45
339	12.57	3	9.6	0.479	5.46	101	−0.90	421	12.91	2	4.0	0.512	.....	100	−0.63	502	13.04	3	5.0	.....	4.41	001	−1.22
341	12.56	3	10.0	0.456	5.44	102	−0.96	422	12.84	3	6.6	0.388	.....	100	−1.24	503	12.99	3	6.9	.....	4.38	001	−1.24
343	12.96	2	3.4	.....	4.11	002	−1.36	423	12.65	1	11.1	0.390	.....	100	−1.28	504	12.96	3	7.7	.....	3.85	001	−1.46
344	12.68	3	5.6	0.408	4.98	101	−1.14	424	12.73	3	11.4	.....	3.90	001	−1.50	505	12.95	3	8.5	.....	5.67	001	−0.75
345	12.67	3	6.2	.....	4.70	001	−1.20	425	12.73	3	16.6	.....	7.03	001	−0.26	507	13.06	3	4.8	.....	5.39	001	−0.83
346	12.73	3	3.5	.....	4.91	001	−1.10	427	12.91	3	4.7	0.385	.....	100	−1.24	508	13.00	3	6.9	.....	3.50	001	−1.58
348	12.58	3	9.6	0.383	4.36	201	−1.34	428	12.90	3	5.1	0.447	.....	100	−0.94	509	12.94	1	8.8	.....	4.37	001	−1.26
350	12.69	3	5.7	0.365	4.15	101	−1.40	429	12.92	2	4.1	0.305	.....	100	−1.61	512	13.04	3	5.9	.....	5.26	001	−0.89
351	12.57	3	10.1	0.372	4.22	101	−1.40	430	12.73	3	12.2	.....	4.09	001	−1.42	513	13.08	3	4.4	.....	7.09	001	−0.14
352	12.61	3	9.0	0.464	5.40	101	−0.94	433	12.99	2	3.7	.....	4.87	001	−1.05	514	13.09	3	3.5	.....	3.85	001	−1.43
354	12.55	3	15.7	0.366	4.12	102	−1.44	434	12.76	1	20.6	.....	4.45	001	−1.28	515	13.06	3	5.1	.....	4.28	001	−1.26
355	12.65	3	7.3	.....	4.01	001	−1.48	435	12.75	3	18.5	.....	3.53	001	−1.63	516	12.91	3	10.7	.....	5.36	001	−0.88
356	12.86	2	3.6	0.334	4.39	101	−1.38	436	12.95	2	4.6	.....	4.61	001	−1.16	517	13.07	3	5.2	.....	7.49	001	0.02
357	12.69	3	6.0	.....	6.81	001	−0.36	437	12.91	3	5.3	.....	4.13	001	−1.36	518	13.04	3	6.0	.....	4.11	001	−1.34
359	12.55	3	13.1	0.433	5.08	101	−1.09	438	12.76	3	11.2	.....	3.93	001	−1.48	520	13.10	3	4.0	.....	4.34	001	−1.23
360	12.75	3	3.8	.....	5.19	001	−0.99	440	12.84	3	8.0	0.419	.....	100	−1.09	521	13.08	3	4.8	.....	4.59	001	−1.14
361	12.61	3	9.2	.....	4.25	001	−1.39	441	12.91	3	5.7	0.362	.....	100	−1.35	522	13.10	3	3.8	.....	5.03	001	−0.96
362	12.59	3	9.8	.....	4.06	001	−1.47	442	12.77	3	14.7	.....	4.12	001	−1.40	523	13.10	3	3.9	.....	6.83	001	−0.24
363	12.57	3	10.9	.....	4.94	001	−1.14	443	12.98	3	3.7	.....	4.04	001	−1.38	526	12.91	3	14.2	.....	3.83	001	−1.48
364	12.50	1	8.4	.....	4.20	001	−1.44	444	12.99	2	4.7	.....	5.14	001	−0.94	529	13.10	3	4.2	.....	3.88	001	−1.41
367	12.68	3	7.3	0.553	6.18	101	−0.55	445	12.92	3	6.2	.....	5.22	001	−0.93	530	13.03	3	6.7	.....	4.70	001	−1.11
368	12.70	3	6.6	.....	3.98	001	−1.47	446	12.75	1	14.4	.....	3.86	001	−1.51	531	13.01	3	7.6	.....	4.13	001	−1.34
369	12.58	3	21.4	.....	4.31	001	−1.38	447	12.80	3	10.5	.....	7.26	001	−0.15	532	13.02	3	7.2	.....	4.57	001	−1.16
370	12.58	3	19.8	0.398	4.99	201	−1.18	448	12.79	3	14.2	.....	3.74	001	−1.54	533	13.05	3	6.4	.....	5.78	001	−0.68
371	12.68	1	8.4	0.543	6.94	101	−0.42	449	12.79	3	12.6	.....	4.20	001	−1.37	534	13.04	3	6.8	.....	4.35	001	−1.24
372	12.76	2	4.8	0.501	5.76	101	−0.74	450	12.94	1	7.4	.....	4.07	001	−1.38	535	13.00	3	8.4	.....	4.08	001	−1.36

taken from the Woolley et al. (1966) catalog, which surveyed the annulus 3′–22′ from cluster center, and these may be identified as three-digit numbers in column (1) of the table. Three series of four-digit identifications are also present in the sample. The 7000 series contains 20 stars from the work of Seitzer (1983) on objects lying farther than ∼22′ from cluster center. While some of these are fainter than $V = 13$, we include them here for their intrinsic interest. The 8000 and 9000 series comprise objects within ∼4′ of cluster center: the 9000 series was identified from short-exposure photographic plates for the present work, while the 8000 series contains objects initially chosen from the chart of Martin (1938, Plate II) for the purposes of an independent radial velocity investigation. Coordinates of the 8000 and 9000 series are presented in Appendix B, while V magnitudes, their sources, and radial distance from cluster center are presented in columns (2)–(4) of Table 1. Details of the sources of the magnitudes are given in Appendix A.

We believe that our sample has been determined without any active bias toward abundance. Two further points, however, are worth making. The first is that the sample becomes incomplete at the faint limit, as is shown in Figure

TABLE 1—*Continued*

Star	V[a]	Ref	r	A(Ca)	W	n[b]	[Ca/H]	Star	V[a]	Ref	r	A(Ca)	W	n[b]	[Ca/H]	Star	V[a]	Ref	r	A(Ca)	W	n[b]	[Ca/H]
(1)	(2)	(3)	(4)	(5)	(6)	(7)	(8)	(1)	(2)	(3)	(4)	(5)	(6)	(7)	(8)	(1)	(2)	(3)	(4)	(5)	(6)	(7)	(8)
537	12.90	1	15.0	.....	4.88	001	−1.07	8097	11.96	2	1.8	.....	5.30	001	−1.15	9093	12.51	2	1.8	0.403	.....	100	−1.25
538	13.13	3	3.9	.....	5.19	001	−0.89	8113	12.27	2	2.9	.....	4.77	001	−1.28	9096	11.83	2	1.1	.....	4.72	001	−1.41
540	12.93	3	14.2	.....	4.90	001	−1.05	8114	12.61	2	3.4	.....	4.61	001	−1.25	9100	12.65	2	2.4	0.373	4.49	101	−1.32
541	12.99	3	9.3	.....	4.70	001	−1.12	8115	11.93	2	3.6	.....	6.03	001	−0.87	9101	12.19	2	2.8	.....	4.29	001	−1.48
543	12.98	1	9.2	.....	3.70	001	−1.51	8141	12.47	2	2.5	.....	4.41	001	−1.36	9102	12.93	2	2.8	0.377	.....	100	−1.27
544	13.00	3	9.3	.....	4.82	001	−1.07	8142	12.12	2	1.8	.....	4.48	001	−1.43	9103	12.38	2	2.4	0.429	.....	100	−1.16
545	13.04	3	7.8	.....	4.89	001	−1.03	8145	12.24	2	2.8	.....	5.32	001	−1.07	9104	12.23	2	2.1	0.420	.....	100	−1.24
548	12.96	3	17.8	.....	3.94	001	−1.42	8146	11.74	2	3.2	.....	5.76	001	−1.02	9105	13.09	2	2.2	0.609	.....	100	−0.10
550	13.08	3	6.7	0.328	3.90	101	−1.44	8148	11.65	2	2.7	.....	5.56	001	−1.13	9106	13.24	2	2.1	0.325	.....	100	−1.44
557	12.97	3	12.0	.....	5.68	001	−0.74	8149	11.54	2	3.7	.....	4.08	001	−1.73	9107	13.00	2	1.9	0.492	.....	100	−0.70
558	13.06	1	9.9	.....	4.31	001	−1.26	8161	12.43	2	3.4	.....	4.69	001	−1.27	9110	13.15	2	0.7	0.293	.....	100	−1.61
570	13.05	3	9.0	.....	3.80	001	−1.46	8162	12.08	2	3.5	.....	4.94	001	−1.26	9111	12.26	2	1.0	.....	4.80	001	−1.27
577	13.16	3	5.4	.....	4.71	001	CH	8181	12.35	2	2.7	.....	4.11	001	−1.51	9113	12.91	2	1.1	0.410	.....	100	−1.12
579	13.03	3	10.1	.....	3.65	001	−1.52	8182	12.25	2	3.2	.....	5.14	002	−1.14	9114	12.94	2	1.4	0.363	.....	100	−1.33
581	13.01	3	11.1	.....	4.06	001	−1.36	8185	12.31	2	1.2	.....	4.34	001	−1.43	9119	12.50	2	2.0	0.394	4.70	101	−1.27
586	13.15	3	5.9	0.420	.....	100	−1.01	8186	13.38	2	3.2	.....	3.57	001	−1.46	9120	12.31	2	2.1	.....	4.33	001	−1.44
7006	12.43	1	22.4	0.446	5.57	201	−0.99	8187	11.44	2	0.8	.....	5.06	001	−1.37	9139	11.56	2	2.1	.....	5.06	001	−1.34
7023	11.60	1	27.0	0.447	5.34	101	−1.25	9002	11.97	2	1.9	.....	5.86	001	−0.93	9148	12.79	2	1.2	0.418	.....	100	−1.11
7052	13.36	1	24.8	0.367	4.20	101	−1.22	9003	12.91	2	2.5	0.339	4.25	101	−1.38	9149	13.11	2	0.8	0.372	.....	100	−1.25
7067	12.64	1	23.0	0.429	4.98	101	−1.10	9004	12.42	2	2.7	0.360	.....	100	−1.48	9154	11.95	2	2.2	.....	6.21	001	−0.79
7102	11.58	1	23.2	0.436	5.14	101	−1.32	9006	11.92	2	2.1	.....	5.26	001	−1.18	9155	12.63	2	2.4	0.489	4.76	101	−1.00
7126	13.14	1	26.6	0.358	3.98	201	−1.33	9007	12.53	2	1.8	0.427	4.67	101	−1.19	9156	12.59	2	2.4	0.463	5.18	101	−0.99
7145	12.70	1	38.4	0.438	5.04	203	−1.05	9008	13.38	2	1.4	0.307	.....	100	−1.49	9157	13.17	2	2.4	0.487	5.97	101	−0.62
7148	13.28	1	30.1	0.281	3.14	201	−1.64	9012	12.51	2	1.1	0.370	3.93	201	−1.47	9159	12.64	2	2.0	0.427	4.96	101	−1.11
7191	13.07	1	25.6	0.330	3.94	201	−1.43	9013	12.60	2	2.0	0.481	5.67	201	−0.85	9167	12.69	2	1.9	0.391	4.76	101	−1.22
7240	13.20	1	31.7	0.316	3.29	201	−1.55	9017	12.87	2	2.6	0.346	3.92	101	−1.44	9173	13.06	2	2.3	0.440	.....	100	−0.94
7242	13.03	1	30.9	0.343	3.88	201	−1.42	9018	13.02	2	2.2	0.431	6.08	101	−0.78	9174	12.64	2	1.9	0.373	4.61	101	−1.30
7251	12.23	1	24.9	0.466	.....	200	−1.02	9019	13.12	2	2.6	0.357	4.13	101	−1.31	9175	12.62	2	1.1	0.293	4.12	101	CH
7299	13.05	1	23.1	0.337	3.84	201	−1.43	9020	13.10	2	2.4	0.415	4.69	101	−1.07	9179	13.43	2	1.3	0.344	.....	100	−1.30
7345	11.77	1	27.5	0.444	.....	200	−1.25	9021	12.60	2	2.2	0.369	4.22	101	−1.40	9183	11.82	2	2.0	.....	4.38	001	−1.54
7359	12.59	1	38.9	0.376	4.05	201	−1.42	9024	12.40	2	2.6	0.488	5.67	101	−0.88	9185	12.45	2	1.7	0.373	4.58	101	−1.36
7554	13.46	1	27.7	0.315	3.79	101	−1.39	9025	12.83	2	2.2	0.358	4.17	101	−1.38	9188	12.96	2	0.3	0.362	.....	100	−1.33
7564	13.78	1	25.8	0.286	.....	100	−1.48	9033	12.98	2	1.2	0.352	.....	100	−1.38	9190	12.74	2	0.9	0.373	4.12	101	−1.37
7632	13.41	1	24.5	0.327	3.82	101	−1.37	9036	12.10	2	1.1	.....	4.33	001	−1.49	9191	13.18	2	1.1	0.322	.....	100	−1.47
7759	13.33	1	43.7	0.322	3.86	201	−1.39	9040	12.73	2	2.8	0.441	.....	100	−1.02	9195	12.41	2	1.8	0.378	.....	100	−1.40
7903	13.46	1	28.6	0.333	4.18	101	−1.27	9042	12.57	2	2.4	0.409	.....	100	−1.21	9196	12.14	2	2.5	.....	5.70	001	−0.94
8002	11.15	2	1.1	.....	4.28	002	−1.75	9063	13.00	2	2.1	0.335	.....	100	−1.45	9197	12.89	2	1.8	0.368	.....	100	−1.32
8006	12.19	2	0.3	.....	4.55	001	−1.38	9066	12.81	3	2.4	0.491	.....	100	−0.75	9201	13.37	2	1.1	0.307	.....	100	−1.49
8041	12.83	2	2.9	.....	3.98	001	−1.44	9068	12.73	2	2.5	0.576	.....	100	−0.36	9202	11.80	2	1.0	.....	4.71	001	−1.42
8042	12.59	2	2.7	.....	4.72	001	−1.21	9069	12.84	2	2.5	0.353	.....	100	−1.41	9203	12.69	2	0.7	0.318	.....	100	−1.61
8043	12.27	2	3.0	.....	5.23	001	−1.09	9070	12.78	2	2.4	0.432	.....	100	−1.05	9206	12.53	2	1.0	0.382	.....	100	−1.35
8044	12.22	2	3.1	.....	6.76	001	−0.50	9073	12.82	2	2.8	0.348	3.68	101	−1.50	9208	12.87	2	2.0	0.335	.....	100	−1.48
8048	12.62	2	1.4	.....	3.89	001	−1.53	9078	12.60	2	1.8	0.344	3.70	101	−1.56	9213	12.35	2	1.5	.....	4.98	001	−1.17
8081	11.73	2	3.2	.....	4.95	001	−1.34	9079	12.94	2	1.5	0.326	3.59	101	−1.54	9215	12.10	2	2.0	.....	4.59	001	−1.39
8082	12.18	2	3.2	.....	4.48	001	−1.41	9084	11.69	2	1.7	.....	4.93	001	−1.36	9227	12.96	2	1.5	.....	5.40	001	−0.85
8091	12.38	2	3.0	.....	5.54	001	−0.95	9085	12.82	2	2.2	0.452	.....	100	−0.94								

[a] References for *V*.—(1) Cannon & Stobie 1973a, Eggen 1972, and Seiter 1983; (2) Lyngå 1995; (3) Woolley et al. 1966 and the present work, transformed as discussed in Appendix A.

[b] Three-digit positional code giving number of observations obtained with AAT (1) and 1.9 m telescope in 1993 (2) and 1993 (3).

1, where, for objects in the Woolley et al. catalog, we present the ratio of stars observed to those on our observing list as a function of *V* magnitude. (Proper-motion and radial velocity nonmembers and non–red giants have been excluded from the determination.) This incompleteness, however, should introduce no abundance bias. (We note that comparison of the 8000 and 9000 series with the work of Lyngå 1995 shows that only ∼30% of giants inside 3′ were observed but with no magnitude bias. Essentially all stars in the Seitzer 1983 sample were observed.) Second, as we shall discuss in § 5.2, the setting of a magnitude limit to the sample naturally introduces a nonnegligible bias against metal-rich objects relative to metal-poor ones.

3. OBSERVATIONAL MATERIAL

Three sets of medium-resolution spectra were obtained over the period 1978–1993 with the Anglo-Australian Telescope (AAT) and the 1.9 m telescope at Mount Stromlo. With the AAT we observed the Ca II H and K lines, while with the 1.9 m telescope we obtained data for the calcium triplet at 8498–8662 Å.

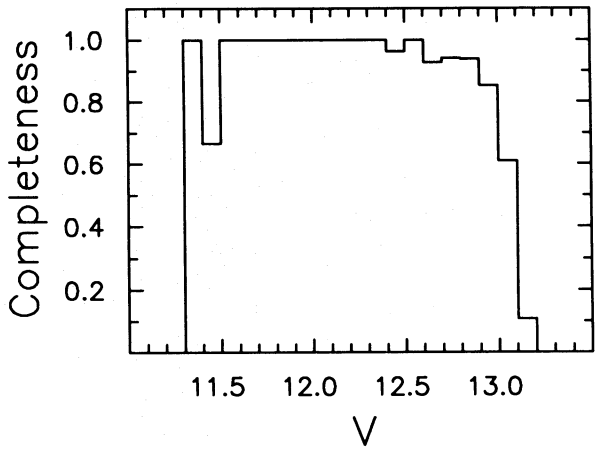

FIG. 1.—Completeness of the present survey as a function of *V* for the Woolley et al. (1966) sample. The completeness is the ratio of stars observed to those in the catalog, excluding proper-motion and radial velocity nonmembers and objects not on the red giant branch.

3.1. *The* Ca II H *and* K *Lines*

Spectra were obtained of some 188 ω Cen red giants with the RGO spectrograph/Image Photon Counting System combination attached to the AAT during observing sessions in 1978 April and 1979 March and May. They cover the wavelength range 3600–4600 Å, with resolution 1.0 Å FWHM, and an average exposure yielded ~100 detected photons per 0.48 Å pixel at 3900 Å. Figure 2*a* presents a typical example of the spectra, for the CN-strong red giant ROA 253. It is perhaps worth noting that the 1978 subset of this material provided the basis of the work reported by Norris (1980).

From these data we measured the Ca abundance indicator A(Ca) defined by Norris et al. (1981) as $A(\mathrm{Ca}) = 1.-2.\bar{I}(3916, 3985)/[\bar{I}(3883, 3916) + \bar{I}(3985, 4018)]$, where $\bar{I}(\lambda_1, \lambda_2) = \int_{\lambda_1}^{\lambda_2} I_\lambda d\lambda/(\lambda_2 - \lambda_1)$ and I_λ is the measured flux at wavelength λ. This parameter is a measure of the mean absorption of the Ca II H and K lines. From stars with repeat observations, the standard error of a single observation is estimated to be 0.009. The A(Ca) values are presented in columns (5) of Table 1.

3.2. *The Calcium Triplet*

During observing sessions in 1992 March–June we used the coudé spectrograph of the 1.9 m telescope to obtain spectra of 206 ω Cen red giants in the wavelength range 8470–8730 Å at 1.4 Å resolution. The detector was a GEC CCD. We also observed as standards red giants in the clusters 47 Tuc, M4, NGC 6397, and NGC 6752, many of which were chosen from the lists of Armandroff & Da Costa (1991, hereafter AD) and Da Costa, Armandroff, & Norris (1992). The average number of detected photons per observation was ~1000 per 0.45 Å pixel.

In 1993 April–June we used the Cassegrain spectrograph attached to the 1.9 m telescope, together with the same CCD detector, to observe some 322 ω Cen objects and a subset of the above standards in the wavelength range 8350–8850 Å, with resolution 3.6 Å. On average we obtained ~1000 detected photons per 0.87 Å pixel per observation. An example of the spectra, again for the CN-strong star ROA 253, is shown in Figure 2*b*.

From these spectra we measured the equivalent widths of the strongest two of the Ca triplet and formed the line strength index $W_{8542} + W_{8662}$ as defined by AD. In what follows we shall refer to this as the calcium triplet index and for convenience shall abbreviate the symbol to W. The results for the standard stars observed with the coudé setup are presented in column (4) of Table 2, together in column (6) with average values from the works of AD and Da Costa et al. (1992), while in Figure 3 the comparison is made between our results and theirs. The agreement between the two data sets is pleasing, although it is clear that at the smallest line strengths our results are systematically larger. Note, however, that for the bulk of our ω Cen sample the triplet index lies in the range 4–6 Å, where the agreement between the present work and those of AD and Da Costa et al. (1992) is very good. From ω Cen stars with multiple observations we estimate the standard error of a single observation to be 0.18 and 0.15 Å for the 1992 and 1993 data sets, respectively.

Figure 4 presents a comparison of the triplet indices measured in both the 1992 and 1993 seasons for ω Cen and calibrating cluster stars. It will be seen that there is a small systematic difference between the two data sets, which is well described by the least-squares line of best fit $[W(1992) = 0.486 + 0.698W(1993) + 0.0447W(1993)^5]$shown in the figure. We use this relation to transform the 1993 data set onto the 1992 system and present our triplet index results, all on the 1992 system, in column (6) of Table 1. We note that in the case of stars that were observed in both seasons, we tabulate the average value, after the transformation has been effected. In column (7) of the table we use a three-digit positional code to present the number of observations obtained of A(Ca) and of W in each of 1992 and 1993.

3.3. *Comparison of A(Ca) and the Triplet Index*

In Figure 5 we compare our results for A(Ca) and W for objects having measurements of both indices. Except for six

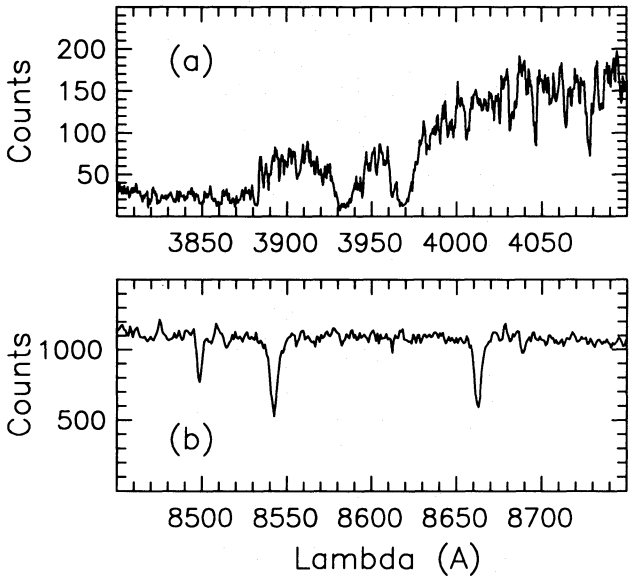

FIG. 2.—Spectra of the CN-strong red giant ROA 253 in the region of (*a*) the Ca II H and K lines and (*b*) the Ca II infrared triplet.

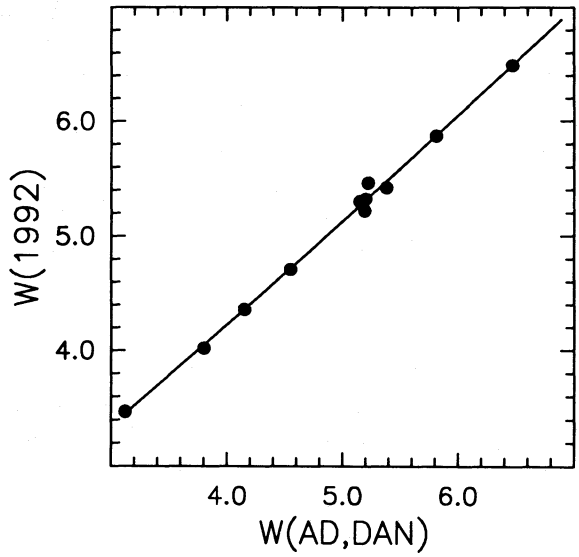

FIG. 3.—Comparison between the present measures of the calcium triplet indices ($W = W_{8542} + W_{8662}$) obtained in 1992 with those of AD and Da Costa et al. (1992). The line is the least-squares quadratic fit to the data.

TABLE 2

GLOBULAR CLUSTER CALIBRATION DATA

Cluster (1)	Object[a] (2)	V[b] (3)	W_{NFM} (4)	n (5)	W_{Other}[c] (6)	V_{HB}[c] (7)	$\langle W' \rangle$ (8)	[Fe/H][d] (9)	[Ca/Fe][d] (10)
47 Tuc	L1510	12.15	6.15	1	...	14.06	5.08	−0.75	0.15
	L2525	12.43	6.49	1	...				
	L3512	11.79	6.49	1	6.47				
	L4418	12.16	6.40	1	...				
	L5529	11.89	6.73	1	...				
	L8517	12.62	5.92	2	...				
M4	L1501	11.63	5.32	6	5.20	13.35	4.23	−1.15	0.20
	L2617	11.90	5.30	3	5.15				
	L4415	12.52	4.71	4	4.55				
	L4613	10.81	5.87	4	5.81				
NGC 6397.....	RGO 211	10.16	4.36	6	4.15	12.90	2.52	−2.00	0.35
	RGO 428	11.50	3.47	5	3.12				
	RGO 669	10.50	4.02	5	3.80				
	RGO 685	12.01	3.08	5	...				
NGC 6752.....	A3	12.02	4.74	3	...	13.95	4.59	−1.55	0.30
	A12	11.25	5.46	6	5.22				
	A31	10.80	5.22	4	5.19				
	A59	10.90	5.42	6	5.38				
	A68	12.02	4.81	3	...				

[a] Nomenclature from Lee 1977b, Lee 1977a, Woolley et al. 1961, and Alcaino 1972 for 47 Tuc, M4, NGC 6397, and NGC 6752, respectively.

[b] From Lee 1977b, Lee 1977a, Cannon 1974, and Cannon & Stobie 1977b for 47 Tuc, M4, NGC 6397, and NGC 6752, respectively.

[c] From AD and Da Costa et al. 1992.

[d] Based on data from Zinn 1985 and Norris & Da Costa 1995.

stars, which are shown as open symbols, the correlation between the two indices is very tight. Two of the discrepant stars, 279 and 9175 (shown as open stars), have very strongly enhanced CH absorption in the range 4300–4400 Å and are probably CH stars.[5] [Without attempting to justify the point, it is our experience that CH-strong giants in globular clusters have abnormally weak Ca II H and K lines for their abundance, driven perhaps by an increase in the effective continuum opacity; we thus suspect that it is the A(Ca) index that leads to the divergence from the general trend.] The other four stars are 330, 332, 9018, and 9155, none of which appears peculiar with respect to CH. While we shall present abundances for these objects, they will be excluded from our analysis. The line in the figure is the least-squares fit to the filled circles in the diagram and is given by $W = 12.21A(\mathrm{Ca}) - 0.26$. We shall use this relation in § 4.2 to transform the A(Ca) measures to the W scale and note that the error of 0.009 in A(Ca) presented above transforms to 0.11 Å in W.

4. ABUNDANCES

4.1. [Ca/H] *from the Calcium Triplet*

The use of the calcium triplet for abundance determination has been well calibrated by AD, whose procedure we follow, with one exception to be described below.

[5] We are not aware of any previous identification of 279 and 9175 as CH stars. Their inclusion in the class brings the number of CH stars brighter than $V = 13$ in ω Cen to six. The other four are ROA 55 (Harding 1962), ROA 70 (Dickens 1972), ROA 577 (J. E. Norris & R. Zinn, unpublished), and the unnumbered star at $(x, y) = (2.39, 4.02)$ on Plate VI of Woolley et al. (1966) (Bond 1975).

Figure 6 presents the dependence of the triplet index W as a function of $\Delta V = V - V_{HB}$, the difference between observed magnitude of the star and that of the horizontal branch (HB) of the cluster, for red giant branch (RGB) stars in the calibrating clusters 47 Tuc, M4, NGC 6397, and NGC 6752. The data used in preparing the figure and their sources are given in Table 2. The lines in Figure 6 all have

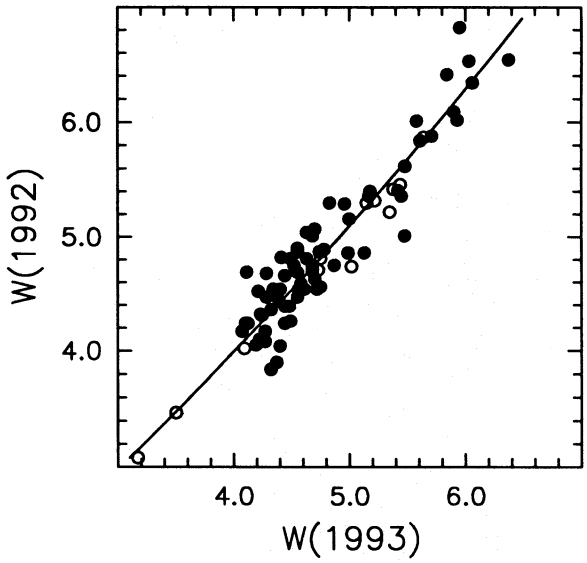

FIG. 4.—Comparison of the calcium triplet indices ($W = W_{8542} + W_{8662}$) obtained in 1992 and 1993. Open and filled symbols refer to calibrating cluster and ω Cen red giants, respectively. The line is the least-squares quadratic fit to the data.

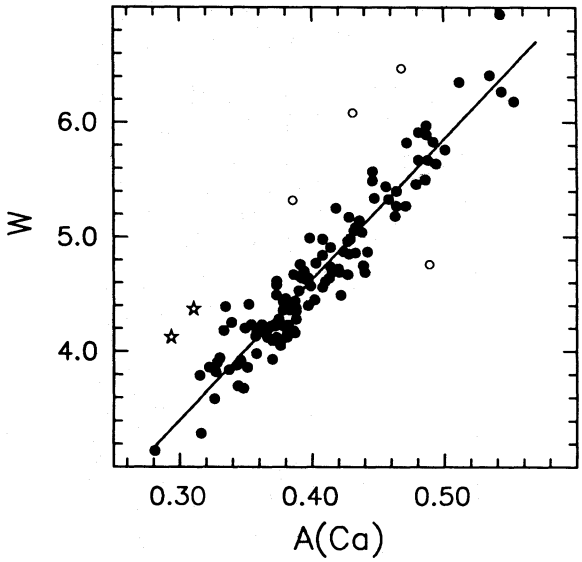

FIG. 5.—Calcium triplet index W ($=W_{8542}+W_{8662}$) vs. the Ca II H and K index A(Ca). The line is the least-squares linear fit to the filled circles. (The open symbols are identified as deviating from the bulk of the sample, with two of them [*open stars*] being CH-strong objects.)

slope −0.654, which represents the weighted mean value of individual determinations of the lines of least-squares best fit for the four clusters. The intercepts in the figure were determined by least-squares minimization of residuals with the slope fixed at this value.

Following AD we define the reduced triplet index $W' = W - 0.654\Delta V$, which effectively represents the index at a common magnitude. At this point AD then plot mean cluster W' versus cluster [Fe/H] to determine the required transformation between W' and abundance, the implicit assumption being that there is a well-determined and unique relationship between calcium and iron in all clusters. While this assumption may be valid for the globular cluster population as a whole (though this remains to be rigorously demonstrated), there is some evidence that calcium has been overproduced in ω Cen and that it does not follow the general behavior found for the other clusters. Inspection of the dependence of [Ca/Fe] on [Fe/H] from the high-dispersion abundance analysis of 40 ω Cen red giants and a number of objects in "normal" clusters by Norris & Da Costa (1995, their Fig. 5) shows that at [Fe/H] ∼ −1, calcium appears to have been overproduced by 0.2–0.3 dex in ω Cen. To address this problem we choose to calibrate [Ca/H], rather than [Fe/H], versus W' for the clusters that we observed (§ 3) and the 40 ω Cen giants analyzed by Norris & Da Costa (1995). For the clusters our adopted values and their sources are presented in Table 2, while for the ω Cen giants we refer the reader to Norris & Da Costa (1995) for the stars involved together with their abundances and to Table 1 for values of W and V. The dependence of [Ca/H] on W' is presented in Figure 7, where the line in the figure is our basic calibration, given by $[Ca/H] = -2.61 - 0.3923W' + 0.00368W'^2$, the least-squares quadratic fit to the data.

In computing W' for the ω Cen giants we have adopted $V_{HB} = 14.84 + 0.25$ [Ca/H], assuming that for the observed mean cluster HB magnitude of $V_{HB} = 14.52$ (Harris 1976) the appropriate mean abundance is [Ca/H] = −1.3 (determined a posteriori from, e.g., Fig. 10) and that dV_{HB}/d[Ca/H] = 0.25 (a compromise between the preferred values of Lee, Demarque, & Zinn 1990, Carney, Storm, & Jones 1992, and Sandage 1993). The abundance calibration is, however, quite insensitive to these assumptions: a change of 0.2 dex in the adopted mean HB abundance leads to Δ[Ca/H] = 0.01 at $W' = 3.5$, which is also the difference caused by a change of 0.05 in dV_{HB}/d[Ca/H]. For the calibrating ω Cen giants, V_{HB} was determined by using the [Ca/H] values of Norris & Da Costa (1995), while for the program stars, we initially assumed [Ca/H] = −1.3 to determine V_{HB}, computed the abundance of the star using the calibration, and then iterated the procedure until the assumed and deduced abundances agreed to within 0.02 dex.

We note in conclusion that errors of $\Delta W = 0.15$ and $\Delta V = 0.2$ (see Appendix A) propagate, typically, to Δ[Ca/H] = 0.05 and 0.06, respectively.

4.2. [Ca/H] *from* A(Ca)

We choose not to calibrate A(Ca) via cluster data as was done for the triplet index but rather to transform the observed values of A(Ca) to W by using the relationship defined in § 3.3 and then to use the triplet formalism of § 4.1. In this manner we obtain [Ca/H] from the Ca II H and K

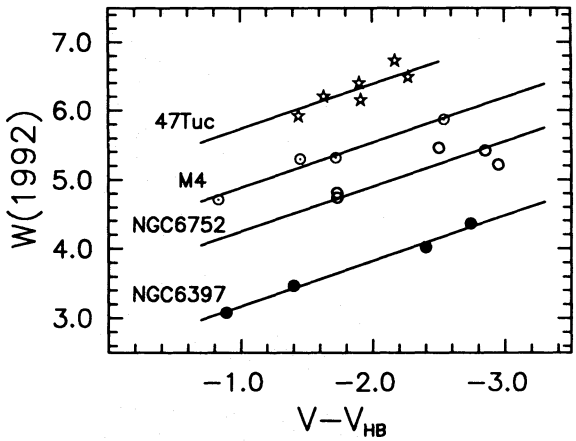

FIG. 6.—Calcium triplet index W ($=W_{8542}+W_{8662}$) as a function of $V-V_{HB}$ for the calibrating clusters 47 Tuc, M4, NGC 6397, and NGC 6752.

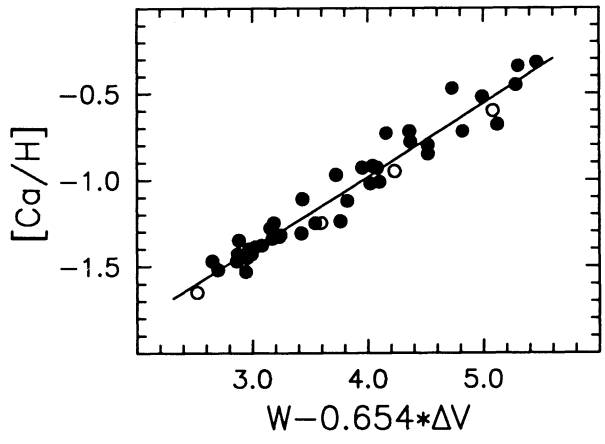

FIG. 7.—Calibration of [Ca/H] as a function of the reduced calcium triplet index $W' = W - 0.654\Delta V$. The open and closed symbols refer to mean calibrating cluster values and to high-resolution abundance results for ω Cen red giants, respectively.

lines on the same system as that determined for the calcium triplet.

4.3. *Homogenized Abundances*

Column (8) of Table 1 presents values of [Ca/H] for 517 ω Cen red giants. (No abundances are given for the four CH stars identified in col. [8] of the table since our calibration is invalid for them.) For objects having only A(Ca) or W, the above transformations lead to the abundances presented in the table. In the case in which both W and A(Ca) exist, we tabulate the average of individual [Ca/H] values, giving equal weight to measures from the three data sets (Ca II H and K and the 1992 and 1993 triplet series). While in this case the A(Ca) and triplet-based abundances are not strictly independent because of the above procedures, we believe that this averaging reduces the random errors of the final values. From stars present in more than one data set, we find the standard error of a single measure of [Ca/H] to be 0.06 dex (having excluded eight stars with greater than 3 σ errors).

The reader will find that six objects in Table 1 have abundances greater than [Ca/H] = −0.2. The abundances for these objects are extrapolations of the calibration shown in Figure 7 and should be treated with caution. The values presented here should be regarded as a first indication and the objects as a source of candidates for future abundance work on this important group of metal-rich objects.

It is of some interest to compare our results with those of high-resolution fine analyses. This is done in Figure 8, where we compare the values in Table 1 with those of Cohen (1981), Gratton (1982), Francois, Spite, & Spite (1988), and Paltoglou & Norris (1989). Vertical lines have been used to connect stars observed by different authors, and the sloping line is the one-to-one relation. Small systematic errors ~0.2–0.3 dex are clearly present between the different data sets, and in general the agreement between our values and the others is satisfactory at this level.

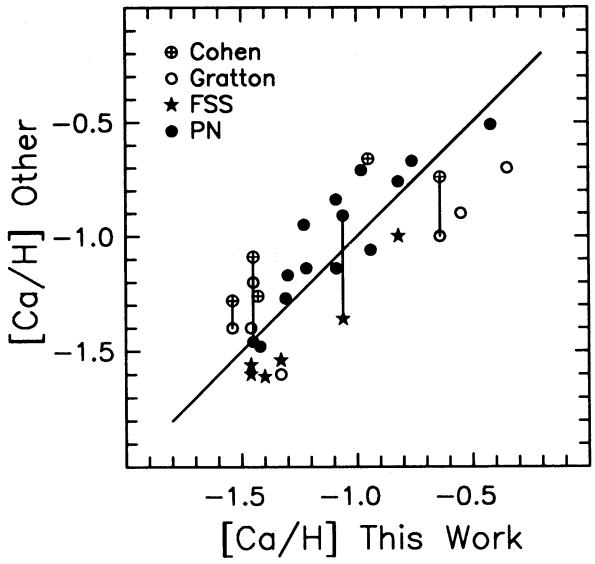

FIG. 8.—Comparison between the calcium abundances obtained in the present work with those of Cohen (1981), Gratton (1982), Francois et al. (1988), and Paltoglou & Norris (1989). Vertical lines join data for the same star, while the sloping line is the one-to-one relation.

5. THE ABUNDANCE DISTRIBUTION

5.1. *Observed* [Ca/H] *Distribution*

In Figures 9*a*–9*c* we present the generalized [Ca/H] distributions of the three data subsets defined by the AAT Ca II H and K material and the 1992 and 1993 calcium triplet measures, respectively. A Gaussian kernel having σ = 0.05

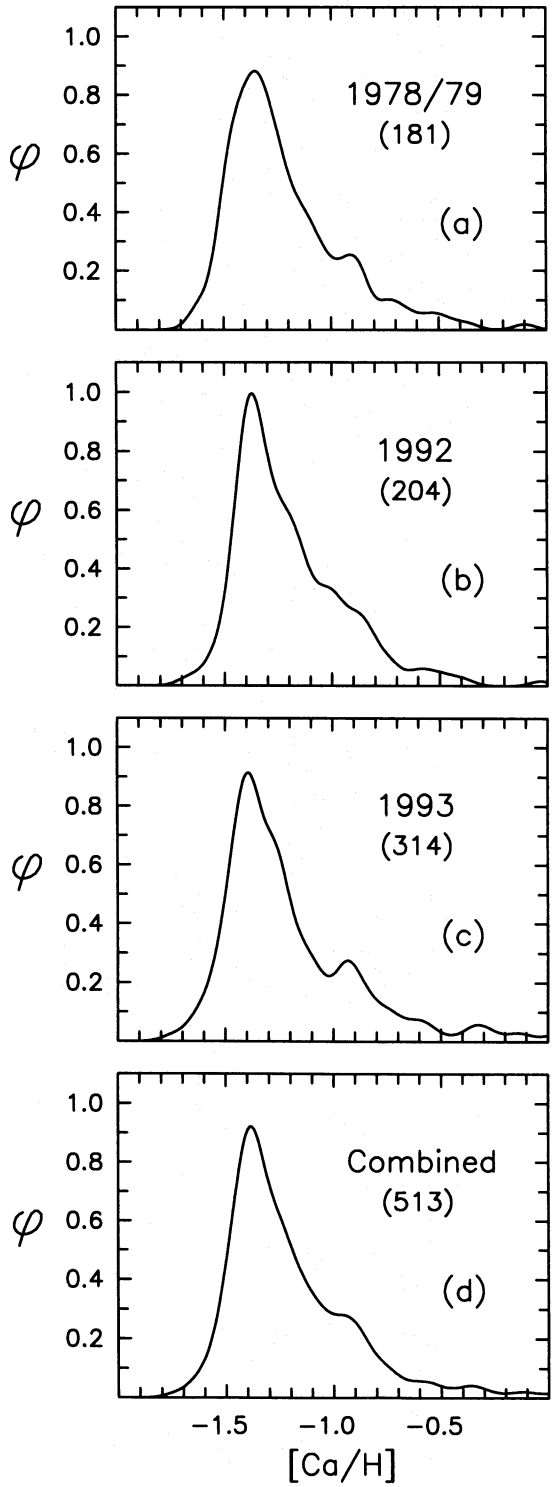

FIG. 9.—Generalized histograms of [Ca/H]: (*a*)–(*c*) for the three individual data sets discussed in the text, and (*d*) for the complete sample of ω Cen red giants. The numbers in parentheses denote the sample sizes. Note the long abundance tail to higher abundance and the secondary peak at [Ca/H] = −0.9.

dex, appropriate to the observational errors discussed above,[6] has been employed. In Figure 9*d* we combine the three samples to show the distribution for the 513 objects in Table 1 that have reliable abundances.

The figure contains the basic observational results of this paper. They are as follows: (1) there are few, if any, stars on the giant branch of ω Cen with [Ca/H] less than −1.60; (2) there is a well-defined peak in the distribution at [Ca/H] = −1.4, with a long tail stretching up to [Ca/H] ∼ −0.3; and (3) the distribution is bimodal with a second peak in the distribution at [Ca/H] = −0.9. Inspection of Figures 9*a*–9*c* shows that these features are present in each of the three independent data sets (with the exception of the bimodality, which is not clear in the 1992 sample but is quite evident in the others), and attests to the reality of the claims. We also note that inspection of the distribution of the complete sample as a function of magnitude reveals differences of the same order as those seen in Figure 9.

It is of interest to compare the present result with the earlier works of Butler et al. (1978), Persson et al. (1980), and Da Costa & Villumsen (1981) referred to in § 1. In general the agreement is excellent concerning points (1) and (2). With respect to point (3), Butler et al. reported a possible bimodality for the abundance distribution of some 37 ab-type RR Lyrae variables that they considered to be of "statistically questionable significance." Given that the apparent bimodality is weakened if the c-type variables are included (see Fig. 4*a* of Persson et al. 1980) and that the RR Lyrae variables form an intrinsically abundance-biased sample, it is difficult to compare our results with theirs, and we choose not to do so. Da Costa & Villumsen (1981) explicitly noted that their distribution was best fitted by two components having mean abundances [Fe/H] = −1.6 and −1.0. We shall see in § 7.1 that we support their conclusion on the need for two such components.

5.2. *Parent* [Ca/H] *Distribution*

It should be appreciated that the distributions of Figure 9 do not necessarily represent the parent distribution of the cluster. There are two considerations.

The first is that the calibration of the triplet index in § 4 assumes that the stars lie on the red giant branch of the cluster, rather than on its asymptotic giant branch (AGB). Indeed, guided by observational and theoretical data on the ratio of AGB to RGB stars (Lee 1977b; Green 1981; Sandage & Katem 1982), one might expect some 20%–40% of the stars in our sample to be AGB stars. The inclusion of such objects causes the following problems. The distribution of AGB stars as a function of abundance may differ from that of objects on their first ascent of the RGB because of the complicated dependence of post-RGB evolution on mass and abundance (see Gingold 1976), which leads to a distortion of the observed distribution. The bluest stars on the horizontal branch may not return to the AGB but rather may evolve into the so-called UV-bright region of the color-magnitude diagram, brighter than the horizontal branch and hotter than the AGB. Since such objects are rare in ω Cen (Norris 1974) and the timescale for their post-HB evolution is of the same order as for those that evolve to the AGB, this is not a significant issue. The accuracy of our abundances for AGB stars should also be examined. Inspection of globular cluster color-magnitude diagrams (see, e.g., Lee 1977b; Sandage & Katem 1982), in the abundance range [Ca/H] = −0.5 to −1.7 considered here, suggests that AGB stars are brighter than RGB stars by up to ∼0.3 mag, which would lead in first approximation to an abundance error of up to ∼0.10 dex for AGB stars under the present formulation. (On average, however, one might expect the error to be more like half this value, since the magnitude difference will lie in the range 0.0–0.3 mag.) Given the absence of recognizable AGB/RGB structure in the observed giant branch of ω Cen (see, e.g., Cannon & Stobie 1973a; Dickens et al. 1988), we are unable to correct for the presence of AGB stars in our sample. However, it seems reasonable, given the above discussion, to suggest that their presence will not seriously affect the observed frequency distribution.

The second, and potentially more important, problem concerns our apparent magnitude cutoff. As noted in § 2, a magnitude-limited sample will be biased since the fraction of stars brighter than any given magnitude is a function of abundance. For example, the work of Green, Demarque, & King (1987) and Straniero & Chieffi (1991) shows that for $Y = 0.23$ and age 14 Gyr, the ratio of the proportion of the parent population brighter than $M_V = -0.9$ and having heavy-element mass fraction $Z = 0.0003$ to that having $Z = 0.003$ is ∼1.3–1.5. Restated in the present context, material at [Ca/H] ∼ −0.7 in Figure 9 will be underrepresented by some 40% relative to that having [Ca/H] ∼ −1.7.

Given the available theoretical luminosity function data, however, this is a tractable problem. One may determine the relative fractions of objects above a given absolute magnitude as a function of abundance and correct the observed distribution for the effect. The result of this procedure is shown in Figure 10, in which we present the corrected histogram, together with the incompleteness function, *R*, that we have applied. The latter is determined from the results of Straniero & Chieffi (1991) for $Y = 0.23$ and age = 14 Gyr and is defined as the fraction of the luminosity function brighter than $M_V = -0.9$ ($V = 13.0$ for ω Cen) normalized to unity for [Ca/H] = −1.8.[7]

6. [Ca/H] AS A FUNCTION OF RADIUS

Dissipative models of chemical enrichment generally predict radial abundance gradients, with higher abundance toward cluster center, and our data suggest that this may indeed have happened in ω Cen. The case for this is made in Figure 11, where in the lower panel we present [Ca/H] as a function of *r*, the distance from cluster center. One notices immediately that the most metal-rich objects appear con-

[6] This represents the mean standard error of the observations, including the effect of those that have multiple observations.

[7] We note the following wrinkle in our determination of the incompleteness function. The results of Straniero & Chieffi (1991) are based on solar abundance ratios, while ω Cen has enhancement of the α elements O, Mg, Si, and Ca (see Norris & Da Costa 1995). To compensate for this shortcoming, we follow Salaris, Chieffi, & Straniero (1993), who demonstrate that one may use isochrones computed with solar abundance ratios to determine those having α enhancement by making an appropriate abundance transformation. In their notation, we adopt an enhancement $f_\alpha = 2.5$ and determine the isochrone behavior for α-enhanced material with heavy-element fraction *Z* by entering the tables of Straniero & Chieffi at $1.96Z$. We also adopt [Ca/H] = log (Z/0.02).

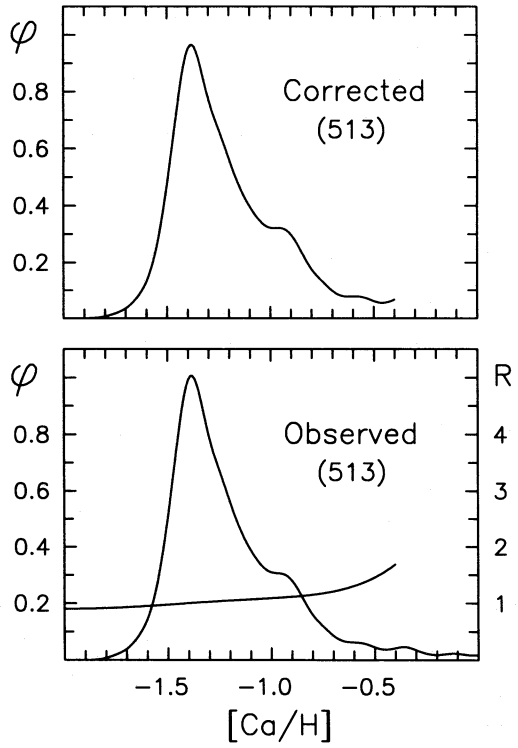

FIG. 10.—Correction of the observed distribution to compensate for the bias introduced by observing a magnitude-limited sample. The lower panel contains the observed distribution, ϕ, together with the theoretical incompleteness correction, R, discussed in the text. The upper panel presents the corrected abundance distribution.

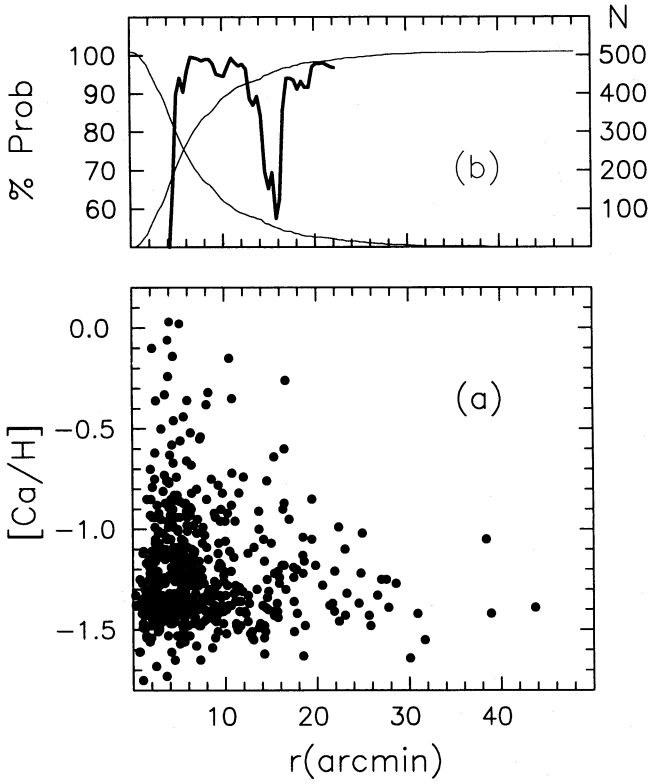

FIG. 11.—(*a*) [Ca/H] as a function of distance from cluster center, r, and (*b*) the probability (*thick line*), based on the one-tailed Mann-Whitney U-test and expressed as a percentage, that two subsamples of the data, one interior and one exterior to radius r, come from different populations, together with the numbers of stars (*thin lines*) involved in the test. See discussion in the text.

centrated toward cluster center and that at distances greater than 20′ there are no objects with [Ca/H] $\gtrsim -1.0$.[8]

It will also be noted, however, that the number of stars is smaller in the outer regions of the cluster, and one might wonder to what extent the effect is only apparent and driven by sample size differences.

In an attempt to quantify the reality of the phenomenon, we split the sample into an inner and an outer subsample and performed a one-tailed Mann-Whitney U-test (Siegel 1956) to ascertain whether the two were drawn from the same population. This test examines whether the bulk of the values of one component is greater than that of the other. The null hypothesis is that the subsamples are the same, while the alternative hypothesis is that the bulk of the inner sample has higher values. Since there is no strongly preferred radius at which to apply the test, we performed it as a function of radius and present the results in the upper panel of Figure 11. (We performed the test only if the sample size was greater than 20 for both subsamples.) The thick line pertains to the ordinate on the left and is a measure of the alternative hypothesis, i.e., the probability (expressed as a percentage) that the samples are different, with the inner subsample having higher values. The numbers of stars in the two subsamples are given by the thin lines, to which the ordinate on the right pertains. These results suggest that for most choices of the dividing radius the two samples are in fact different at greater than the 90% level, the exception being the interval $14' < r < 17'$. An alternative approach to the question is to divide the sample into a number of radially selected groups and to test for differences between the subsamples. Accordingly, we split the sample into three, defined by $r < 10'$, $10' \leq r < 20'$, and $r \geq 20'$. We find that the intermediate sample differs from the innermost one only at the 83% level, while the outermost one differs from the innermost one at the 98% level. These tests collectively suggest to us that the outermost regions ($r \geq 20'$) of ω Cen do indeed differ significantly from its innermost ones, as inspection of Figure 11 indicates.

One might enquire as to whether an initial abundance gradient could survive until the present epoch. According to Djorgovski (1993) the relaxation times for ω Cen at cluster center and half-light radius ($\sim 5'$; Trager, Djorgovski, & King 1993) are both ~ 5 Gyr. Given that relaxation time will increase outside the half-light radius because of the rapidly decreasing density, it seems to us not unreasonable that a metal-rich component initially confined to cluster center should still be identifiable.

7. DISCUSSION

In what follows we shall assume that the distinctive frequency and spatial distributions of [Ca/H] result from phenomena primordial to the cluster rather than to evolutionary mixing phenomena. Support for such a view comes from the fact that [Ca/Fe] is flat as a function of [Fe/H] (Norris & Da Costa 1995), consistent with the production of both elements by massive supernovae during the protocluster phase. Further, no canonical stellar evolution models synthesize calcium in stars of the mass of present-day red giants in ω Cen, which might conceivably be mixed

[8] A similar result has been claimed by J. Norris, K. C. Freeman, & P. Seitzer (unpublished; see Fig. 2 of Freeman & Norris 1981) for the behavior of CN in this cluster.

into the outer layers of these objects prior to their reaching the upper giant branch.

7.1. *Comparison with Simple Enrichment Models*

One of the simplest models of cluster enrichment considers the evolution of a cloud of gas having initial abundance Z_0, which experiences instantaneous recycling of the ejecta from massive supernovae, and from which gas is expelled at a rate proportional to the star formation rate (Searle & Sargent 1972; Hartwick 1976; Zinn 1978). Hartwick (1976) used this model to explain the form of the Galactic globular cluster distribution, while Zinn (1978) applied it to the Draco dwarf spheroidal galaxy. Under these assumptions the form of the abundance distribution is

$$f(Z) = [1/(\langle Z\rangle - Z_0)] \exp [-(Z - Z_0)/(\langle Z\rangle - Z_0)]$$

for $Z \geq Z_0$, where $\langle Z\rangle$ is the mean abundance, and

$$f(Z) = 0$$

for $Z < Z_0$.

We consider the relevance of this distribution to the observations. While the model indeed possesses a long tail to higher abundance, it is incapable of fitting one having the bimodal form seen in Figure 10. The observational material is, however, suggestive of a two-component model, in which one might envisage the components being distinct either in space or in time. We therefore performed a maximum likelihood analysis (see, e.g., Morrison, Flynn, & Freeman 1991 [their Appendix B(c)]) of the data but excluding stars with [Ca/H] > -0.5, in terms of the distribution

$$\begin{aligned} f(Z) = {} & [1/(\langle Z_1\rangle - Z_{10})] \\ & \times \exp [-(Z - Z_{10})/(\langle Z_1\rangle - Z_{10})] \\ & + \beta[1/(\langle Z_2\rangle - Z_{20})] \\ & \times \exp [-(Z - Z_{20})/(\langle Z_2\rangle - Z_{20})] , \end{aligned}$$

where the subscripts 1 and 2 refer to the major and minor components, β is the ratio of the numbers of stars that they contain, and we note that the model was convolved with the observational errors presented above. We began by treating the fit in terms of five free parameters—Z_{10}, $\langle Z_1\rangle$, Z_{20}, $\langle Z_2\rangle$, and β, but experience soon suggested that we fix Z_{10} to correspond to [Ca/H] $= -1.50$, given the sharp low-abundance cutoff of the data and assuming as before [Ca/H] = log (Z/0.02). The best-fit corresponding parameters then are $\langle$[Ca/H]$_1\rangle = -1.28 \pm 0.01$, [Ca/H]$_{20} = -1.05 \pm 0.00$, $\langle$[Ca/H]$_2\rangle = -0.82 \pm 0.03$, and $\beta = 0.17 \pm 0.02$.[9] Comparison between the model and the observations is presented in Figure 12. We note also that it follows from our discussion of the gradient in § 7.1 that the more metal-rich component is more centrally concentrated toward cluster center than the predominant more metal-poor one.

[9] A referee inquired as to how much of an improvement the two-component model was over the alternative single-component one. Setting Z_0 to correspond to [Ca/H] $= -1.50$ as before, we find $\langle$[Ca/H]$\rangle = -1.16$ from maximum likelihood analysis for a single-component model. We then applied the Kolmorov-Smirnov one-sample test (Siegel 1956) to ascertain whether the data are consistent with the model. The test rejects the null hypothesis at the 0.2 significance level (the highest level for which Siegel tabulates critical values). In comparison, it accepts the null hypothesis that the data are consistent with the above two-component model at better than the 0.01 significance level (the lowest value for which Siegel tabulates critical values).

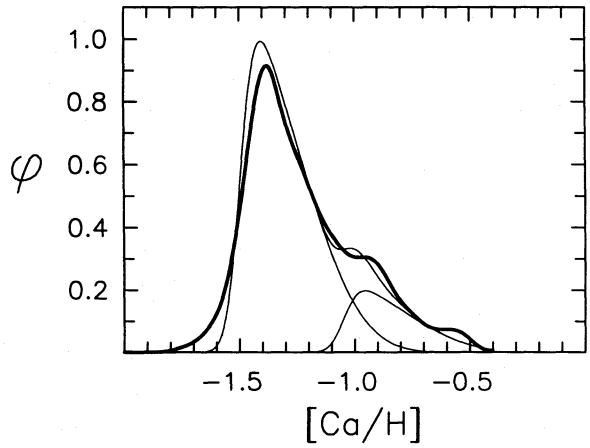

FIG. 12.—Comparison of the ω Cen abundance distribution, corrected for magnitude-limited incompleteness and for stars with [Ca/H] < -0.5, with the two-component simple model distribution discussed in the text. The thick line refers to the observations, while the thin lines show the two individual components and their summation.

7.2. *Proto–ω Centauri*

The material presented here and by Norris & Da Costa (1995) provide a framework within which one may speculate on the early evolution of ω Cen.

7.2.1. *Initial Abundance*

The first question that one might like to address is its initial abundance. The available data demonstrate that there is essentially no material with [Ca/H] < -1.6 in the cluster and that the low-abundance regime of the observed distribution is reasonably well fitted by a simple model having initial abundance [Ca/H] $= -1.5$. While one is by definition unable to rule out the suggestion of Cayrel (1986) that globular clusters condense from metal-free material in which no low-mass zero-metal stars formed, the data are consistent with the view that ω Cen evolved from a cloud having [Ca/H] ~ -1.5.

7.2.2. *Initial Mass*

The large ranges in the abundances of such elements as Mg, Ca, and Fe require that supernovae played an important role in the enrichment of the system and have implications for the mass of the protocloud. Dopita & Smith (1986) argued that 40 supernova explosions were necessary to explain the abundances of Mg and that the cluster must have had a mass greater than $1.8 \times 10^8\ M_\odot$ to prevent the disruption of the system. The more recent analysis of Morgan & Lake (1989), who included more cooling processes in their analysis than did Dopita & Smith, suggests that the present-day mass of ω Cen ($3 \times 10^6\ M_\odot$) is sufficient to have prevented disruption. Obviously, larger protocluster masses are not excluded. The present data add little to these arguments, except perhaps to refine the amount of heavy elements that needs to have been produced. If one accepts that the initial abundance in ω Cen was [Ca/H] $= -1.5$, that [Mg/Ca] $= 0.$ for all values of [Ca/H] (Norris & Da Costa 1995), that log $(N_{\rm Mg}/N_{\rm H})_\odot = -4.46$ (Anders & Grevesse 1989), and that our abundance distribution is characteristic of the $3 \times 10^6\ M_\odot$ of the cluster, one finds that some 80 $M_\odot$ of Mg have been produced within the system. Assuming with Dopita & Smith (1986) that a typical supernova produces 0.3 $M_\odot$ of Mg, the observed abundances imply enrichment by some 270 supernovae. This,

together with the results of Morgan & Lake (1989, their Fig. 4), then implies that a minimum initial cloud mass of $\sim 3 \times 10^6\ M_\odot$ was sufficient to have prevented disruption of the cluster. (It is also of some interest to note that for functions having slopes $x = 0.5$–2.5 [where $d\phi(M)/dM \propto M^{-(1+x)}$], lower and upper limits to stellar masses of 0.15 and 50 $M_\odot$, and a lower limit to the mass of heavy-element–producing supernovae of 10 $M_\odot$, the corresponding total masses of zero-age main-sequence stars are 1×10^4–$2 \times 10^6\ M_\odot$. Insofar as the above formulation of the mass function is appropriate to proto–ω Cen, comparison with the present-day mass thus favors a steep initial mass function for the system.)

A different approach to the initial mass of the system is to assume that the model fit seen in Figure 12 gives a rough approximation to its formation history, in which the system lost matter at a rate proportional to that of star formation. In the simple model discussed above, the fraction of material lost from the system is given by $m_l = 1. - (\langle Z \rangle - Z_0)/y$, where y is the yield and $\langle Z \rangle$ and Z_0 are the mean and initial cluster abundances (Zinn 1978). As noted by Zinn, estimates of the yield vary, but it is "thought to be in the neighborhood of the solar metal abundance." For the purposes of a rough estimate of the mass lost, we ignore the minority component and adopt $\langle [Ca/H] \rangle = -1.3$, $[Ca/H]_0 = -1.5$, and $[Ca/H] = \log(Z/0.02)$. Then for $y = 0.02$ we find that 98% of the protocluster was driven out during the protocluster phase. (If one were to adopt $\langle [Ca/H] \rangle = -1.0$, or $y = 0.005$, this changes to 93%.) For comparison we note that Zinn (1978), in applying this formulation to the Draco dwarf spheroidal galaxy, reported $m_l = 0.99$.

As described by Gunn (1980) such large mass losses are problematic, since they imply that for the cluster to have remained bound following mass loss it must have been 10–100 times smaller initially than it is now. As noted by him, one possible solution to the problem is that the yield may have been smaller (say $y \sim 0.001$) in the protocluster.

7.2.3. *Two Components?*

If one accepts that a two-component model is appropriate to ω Cen as suggested in § 7.1, the question arises as to whether the components were separate in space or in time. On the one hand, one might envisage with Searle (1977) that the cluster may have resulted from the merger of two independent components, while on the other hand, one might postulate two epochs of star formation separated by a hiatus in time, as happened, for example, in the Carina dwarf spheroidal galaxy (Mighell 1990; Smecker-Hane et al. 1994; Smecker-Hane, Stetson, & Hesser 1995). In the latter case one would naturally expect that the second component would be chemically enriched by heavy elements synthesized in the first. In the former scenario, in contradistinction, one would expect no connection between the abundance patterns of the two components.

We believe that the abundances of the heavy elements in ω Cen presented by Norris & Da Costa (1995) and the abundance distribution presented here are together supportive of the two components having been formed at different times during the evolution of the protocluster. A comparison of the two data sets is presented in Figure 13. The upper panel shows the dependence of [Ba/Fe] on [Ca/H] in ω Cen together with the dependence found in other globular clusters, from Norris & Da Costa (1995).

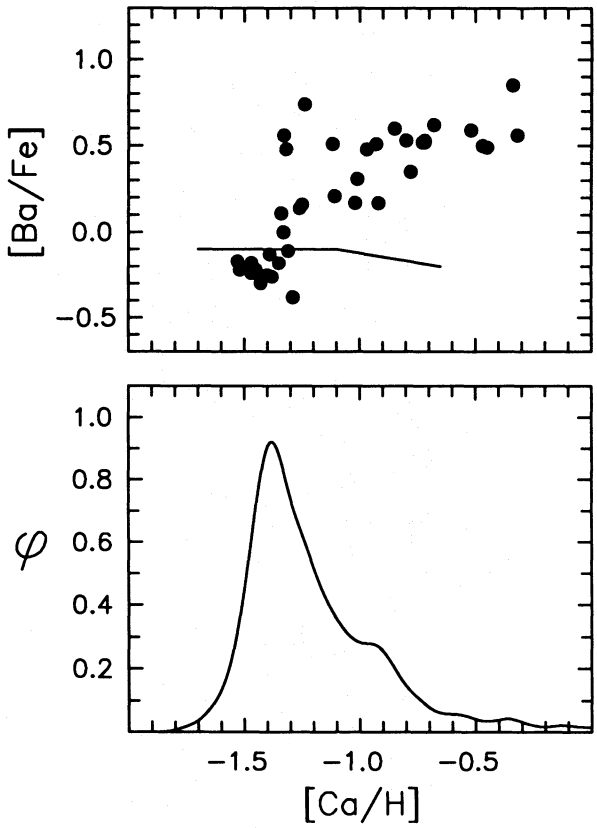

FIG. 13.—Comparison between the observed abundance distribution for ω Cen (*lower panel*) and the dependence of [Ba/Fe] on [Ca/H] (*upper panel*). The points in the upper panel refer to individual stars in ω Cen, while the line represents the behavior found in "normal" clusters, following Norris & Da Costa (1995).

Note the overproduction of Ba relative to Fe in ω Cen relative to the "normal" clusters, which Norris & Da Costa (1995) suggest is driven by primordial enrichment by intermediate-mass stars in ω Cen but which was not experienced in the "normal" clusters. Vanture et al. (1994) have reached the same conclusion concerning the elements Rb, Y, and Zr in ω Cen. In the lower panel of the figure, we present the observed distribution of [Ca/H].

Examination of Figure 13 suggests that the more metal-rich component of the cluster possesses an overproduction of Ba relative to Fe, making it unique among the globular cluster population. We suggest that economy of hypothesis argues against the merger model, since in this case one would be required to ascribe two distinctive features not found elsewhere in the halo to the more metal-rich fragment: not only would it have partaken in the only distinguishable merger observed in the cluster population, but its relative *s*-process overabundance would require it also to have a chemical history different from that of all other globular cluster material. It seems to us much more likely that the *s*-process overproduction in the more metal-rich component in ω Cen is related to the ejecta from an earlier generation in the cluster.

7.2.4. *Duration and Place of Formation*

A final point that follows from the suggestion that ω Cen has produced much of its own *s*-process elements is that evolution of the protocluster occurred over an extended period, $\sim 10^9$ yr. (This follows from the result of Vanture et al. 1994 and Norris & Da Costa 1995 that stars of mass ~ 2

$M_\odot$ were probably involved in the enrichment.) If this were indeed the case, it argues for the cluster forming in isolation from the dense central regions of the young Galaxy, for if it were to have passed though gaseous regions associated with an existing bulge and disk, its gas would have been efficiently stripped during the passage, terminating the enrichment process. The simplest resolution of this problem is that ω Cen evolved within the Searle & Zinn (1978) paradigm of the formation of the Galactic globular cluster system as an independent fragment that later came into dynamical equilibrium with the rest of the Galaxy.

The Sagittarius dwarf spheroidal galaxy and its possibly associated globular cluster M54 (see Ibata, Gilmore, & Irwin 1994; Sarajedini & Layden 1995; and Da Costa & Armandroff 1995) may be an example of the formation and capture process envisaged here. In this context it is important to note that Sarajedini & Layden and Da Costa & Armandroff both report a spread in the abundance of the heavy elements in M54, making it the third such cluster in the Galaxy with this property, following ω Cen and M22. In this same vein, the nucleated dwarf elliptical galaxies may be examples of Searle & Zinn fragments that formed globular cluster–like nuclei, in some cases as luminous as ω Cen, but that managed to evade capture by a larger galaxy (see, e.g., Freeman 1993).

It is a pleasure to thank the Director and staff of the Anglo-Australian Observatory for the use of their facilities. Gosta Lyngå very kindly made his results available to us in advance of publication, together with an electronic version of his catalog. We acknowledge numerous helpful discussions with Professor A. W. Rodgers over the past two decades. His comments and those of G. S. Da Costa on an early version of this work have led to substantial improvements.

APPENDIX A

MAGNITUDES

Visual magnitudes have been determined from the photographic work of Woolley et al. (1966), the photoelectric work of Eggen (1972), Cannon & Stobie (1973a), and Seitzer (1983), and the CCD work of Lyngå (1995). Lyngå noted that the photographic magnitudes of Woolley et al. appear too bright by 0.25 mag toward cluster center, as is shown in Figure 14 in which the difference between CCD or photoelectric magnitude, on the one hand, and photographic magnitude, on the other, is plotted as a function of distance from cluster center. The filled and open symbols denote CCD and photoelectric results, respectively. The reader will note that in the range 6′–10′ the photoelectric results suggest the need for a radial-dependent correction, supporting Lyngå's contention. In determining the V magnitudes presented in Table 1, we have proceeded as follows. If photoelectric or CCD magnitudes exist, these were adopted and averaged in the case of duplicate photoelectric results. When only photographic values exist, they were corrected by $+0.25$ mag for $r < 4'$, $-0.0286r + 0.364$ mag for $3' < r < 11'$, and $+0.05$ mag for $r > 11'$, defined by the lines in Figure 14. In one case (star 9066) the magnitude is based on a photographic value determined for the present work.

APPENDIX B

COORDINATES

The coordinates for the 8000 and 9000 series are presented in Table 3, for epoch 2000, together with cross-identifications to the work of Lyngå (1995). The coordinates are those of Lyngå and are estimated to be accurate to $\sim 1''$. For star 9066 the position comes from the present work.

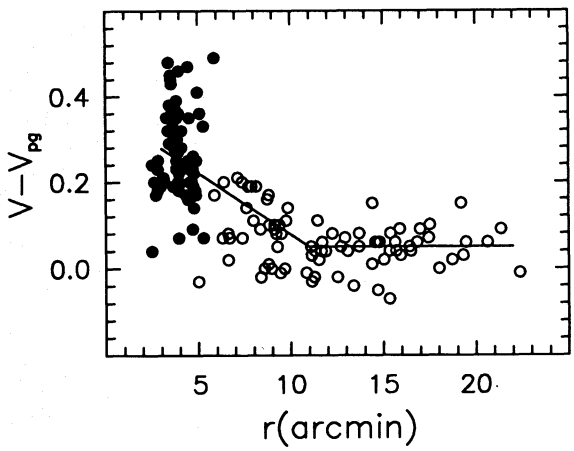

FIG. 14.—Dependence of $\Delta V = V$(CCD, photoelectric) $- V$(photographic) on distance from cluster center for ω Cen. Filled and open symbols refer to CCD and photoelectric data, respectively. The line in the diagram defines the correction that been applied to the photographic data.

TABLE 3

COORDINATES (J2000) FOR ω CENTAURI GIANTS

Star	Lyngå	α	δ	Star	Lyngå	α	δ	Star	Lyngå	α	δ
8002	1367	13 26 43.6	−47 29 35	9013	1826	13 26 49.7	−47 26 45	9113	1879	13 26 50.3	−47 29 30
8006	1449	13 26 44.8	−47 28 29	9017	2016	13 26 52.1	−47 26 17	9114	2068	13 26 52.7	−47 29 34
8041	1078	13 26 39.9	−47 25 55	9018	1981	13 26 51.6	−47 26 38	9119	2317	13 26 55.9	−47 29 56
8042	1132	13 26 40.6	−47 26 08	9019	2109	13 26 53.3	−47 26 22	9120	2237	13 26 54.9	−47 30 14
8043	830	13 26 36.8	−47 26 09	9020	2118	13 26 53.4	−47 26 31	9139	1295	13 26 42.6	−47 30 42
8044	648	13 26 34.2	−47 26 18	9021	2058	13 26 52.6	−47 26 42	9148	1435	13 26 44.6	−47 29 45
8048	1178	13 26 41.2	−47 27 29	9024	2205	13 26 54.5	−47 26 22	9149	1483	13 26 45.3	−47 29 24
8081	2608	13 26 59.6	−47 26 19	9025	2195	13 26 54.3	−47 26 52	9154	1163	13 26 41.0	−47 30 36
8082	2881	13 27 03.4	−47 27 18	9033	1984	13 26 51.6	−47 27 48	9155	1164	13 26 41.0	−47 30 49
8091	2872	13 27 03.4	−47 27 36	9036	1985	13 26 49.2	−47 28 04	9156	1098	13 26 40.1	−47 30 47
8097	2348	13 26 56.3	−47 29 13	9040	2609	13 26 59.6	−47 26 58	9157	1039	13 26 39.4	−47 30 44
8113	2728	13 27 01.1	−47 30 06	9042	2550	13 26 58.6	−47 27 29	9159	1019	13 26 39.1	−47 30 15
8114	2886	13 27 03.5	−47 30 24	9063	2502	13 26 58.1	−47 27 57	9167	909	13 26 37.8	−47 29 46
8115	2812	13 27 02.5	−47 31 02	9066		13 27 00.6	−47 27 29	9173	608	13 26 33.6	−47 29 18
8141	674	13 26 34.5	−47 30 11	9068	2653	13 27 00.3	−47 27 41	9174	748	13 26 35.7	−47 29 11
8142	1197	13 26 41.4	−47 30 12	9069	2693	13 27 00.8	−47 27 52	9175	1095	13 26 40.2	−47 28 51
8145	784	13 26 36.2	−47 30 53	9070	2668	13 27 00.5	−47 28 01	9179	987	13 26 38.8	−47 28 44
8146	574	13 26 33.1	−47 30 57	9073	2843	13 27 02.9	−47 28 03	9183	683	13 26 34.7	−47 28 30
8148	1076	13 26 39.8	−47 31 06	9078	2423	13 26 57.1	−47 28 27	9185	823	13 26 36.7	−47 28 26
8149	733	13 26 35.4	−47 31 46	9079	2250	13 26 55.2	−47 28 35	9188	1540	13 26 46.0	−47 28 23
8161	360	13 26 30.4	−47 30 44	9084	2369	13 26 56.6	−47 28 41	9190	1248	13 26 42.1	−47 28 06
8162	324	13 26 29.9	−47 30 47	9085	2584	13 26 59.2	−47 28 38	9191	1192	13 26 41.5	−47 27 59
8181	397	13 26 30.9	−47 27 59	9093	2375	13 26 56.7	−47 28 60	9195	847	13 26 37.0	−47 27 54
8182	144	13 26 27.3	−47 28 28	9096	2067	13 26 52.7	−47 28 56	9196	604	13 26 33.6	−47 27 33
8185	2046	13 26 52.4	−47 27 59	9100	2624	13 26 59.8	−47 29 35	9197	865	13 26 37.3	−47 27 40
8186	986	13 26 38.8	−47 25 43	9101	2695	13 27 01.1	−47 29 56	9201	1308	13 26 42.9	−47 27 45
8187	1666	13 26 47.7	−47 29 26	9102	2695	13 27 00.8	−47 29 60	9202	1352	13 26 43.4	−47 27 51
9002	1755	13 26 48.8	−47 26 49	9103	2575	13 26 59.1	−47 29 49	9203	1476	13 26 45.1	−47 28 02
9003	1754	13 26 48.8	−47 26 09	9104	2454	13 26 57.5	−47 29 32	9206	1448	13 26 44.8	−47 27 43
9004	1868	13 26 50.2	−47 25 58	9105	2447	13 26 57.4	−47 29 47	9208	856	13 26 37.1	−47 27 23
9006	1809	13 26 49.5	−47 26 33	9106	2376	13 26 56.7	−47 29 51	9213	1178	13 26 41.2	−47 27 29
9007	1777	13 26 49.1	−47 26 55	9107	2301	13 26 55.7	−47 29 47	9215	1113	13 26 40.4	−47 26 57
9008	1719	13 26 48.2	−47 27 21	9110	1837	13 26 49.8	−47 29 09	9227	1559	13 26 46.4	−47 27 02
9012	1778	13 26 49.1	−47 27 39	9111	1953	13 26 51.2	−47 29 16				

REFERENCES

Alcaino, G. 1972, A&A, 16, 220
Anders, E., & Grevesse, N. 1989, Geochim. Cosmochim. Acta, 53, 197
Armandroff, T. E., & Da Costa, G. S. 1991, AJ, 101, 1329 (AD)
Bond, H. E. 1975, ApJ, 202, L47
Brown, J. A., & Wallerstein, G. 1993, AJ, 106, 133
Butler, D., Dickens, R. J., & Epps, E. 1978, ApJ, 225, 148
Cannon, R. D. 1974, MNRAS, 167, 551
Cannon, R. D., & Stobie, R. S. 1973a, MNRAS, 162, 207
———. 1973b, MNRAS, 162, 227
Carney, B. W., Storm, J., & Jones, R. V. 1992, ApJ, 386, 663
Cayrel, R. 1986, A&A, 168, 81
Cohen, J. G. 1981, ApJ, 247, 869
Da Costa, G. S., & Armandroff, T. E. 1995, AJ, 109, 2533
Da Costa, G. S., Armandroff, T. E., & Norris, J. E. 1992, AJ, 104, 154
Da Costa, G. S., & Villumsen, J. E. 1981, in Astrophysical Parameters for Globular Clusters, ed. A. G. D. Philip & D. S. Hayes (Schenectady: Davis), 527
Dickens, R. J. 1972, MNRAS, 159, 7P
Dickens, R. J., Brodie, I. R., Bingham, E. A., & Caldwell, S. P. 1988, SERC Rutherford Appleton Laboratory, RAL-88-004
Djorgovski, S. 1993, in ASP Conf. Proc. 50, Structure and Dynamics of Globular Clusters, ed. S. G. Djorgovski & G. Meylan (San Francisco: ASP), 373
Dopita, M. A., & Smith, G. H. 1986, ApJ, 304, 283
Eggen, O. J. 1972, ApJ, 172, 639
Francois, P., Spite, M., & Spite, F. 1988, A&A, 191, 267
Freeman, K. C. 1993, in ASP Conf. Proc. 48, The Globular Cluster–Galaxy Connection, ed. G. H. Smith & J. P. Brodie (San Francisco: ASP), 608
Freeman, K. C., & Norris, J. 1981, ARA&A 19, 319
Freeman, K. C., & Rodgers, A. W. 1975, ApJ, 201, L71
Gingold, R. A. 1976, ApJ, 204, 116
Gratton, R. G. 1982, A&A, 115, 336
Green, E. M. 1981, Ph.D. thesis, Univ. of Texas
Green, E. M., Demarque, P., & King, C. R. 1987, The Revised Yale Isochrones and Luminosity Functions (New Haven: Yale Univ. Obs.)
Gunn, J. E. 1980, in Globular Clusters, ed. D. Hanes & B. Madore (Cambridge: Cambridge Univ. Press), 301
Harding, G.A. 1962, Observatory, 82, 205
Harris, W. E. 1976, AJ, 81, 1095
Hartwick, F. D. A. 1976, ApJ, 209, 418
Ibata, R. A., Gilmore, G., & Irwin, M. J. 1994, Nature, 370, 194
Kraft, R. P. 1979, ARA&A, 17, 309
———. 1994, PASP, 106, 553
Lee, S.-W. 1977a, A&AS, 27, 367
Lee, S.-W. 1977b, A&AS, 27, 381
Lee, Y.-W., Demarque, P., & Zinn, R. 1990, ApJ, 350, 155
Lyngå, G. 1995, A&A, submitted
Martin, W. C. 1938, Leiden Ann., 17
Mighell, K. J. 1990, A&AS, 82, 1
Morgan, S., & Lake, G. 1989, ApJ, 339, 171
Morrison, H. L., Flynn, C., & Freeman, K. C. 1991, AJ, 100, 1191
Norris, J. 1974, ApJ, 194, 109
———. 1980, in Globular Clusters, ed. D. Hanes & B. Madore (Cambridge: Cambridge Univ. Press), 113
Norris, J., & Bessell, M. S. 1975, ApJ, 201, L75
Norris, J., Cottrell, P. L., Freeman, K. C., & Da Costa, G. S. 1981, ApJ, 244, 205
Norris, J. E., & Da Costa, G. S. 1995, ApJ, 447, 680
Paltoglou, G., & Norris, J. E. 1989, ApJ, 336, 185
Persson, S. E., Frogel, J. A., Cohen, J. G., Aaronson, M., & Matthews, K. 1980, ApJ, 235, 452
Salaris, M., Chieffi, A., & Straniero, O. 1993, ApJ, 414, 580
Sandage, A. 1993, AJ, 106, 719
Sandage, A., & Katem, B. 1982, AJ, 87, 537
Sarajedini, A., & Layden, A. C. 1995, AJ, 109, 1086
Searle, L. 1977, in The Evolution of Galaxies and Stellar Populations, ed. B. M. Tinsley & R. B. Larson (New Haven: Yale Univ. Obs.), 219
Searle, L., & Sargent, W. L. W. 1972, ApJ, 173, 25
Searle, L. & Zinn, R. 1978, ApJ, 225, 357
Seitzer, P. 1983, Ph.D. thesis, Univ. of Virginia
Siegel, S. 1956, Nonparametric Statistics for the Behavioral Sciences (Tokyo: McGraw-Hill Kogakuska)
Smecker-Hane, T. A., Stetson, P. B., & Hesser, J. E. 1995, BAAS, 26, 1396
Smecker-Hane, T. A., Stetson, P. B., Hesser, J. E., & Lehnert, M. D. 1994, AJ, 108, 507
Smith, G. H. 1987, PASP, 99, 67
Straniero, O., & Chieffi, A. 1991, ApJS, 76, 525
Suntzeff, N. 1993, in ASP Conf. Proc. 48, The Globular Cluster–Galaxy Connection, ed. G. H. Smith & J. P. Brodie (San Francisco: ASP), 167
Trager, S. C., Djorgovski, S., & King, I. R. 1993, in ASP Conf. Proc. 50, Structure and Dynamics of Globular Clusters, ed. S. G. Djorgovski & G. Meylan (San Francisco: ASP), 347
Vanture, A. D., Wallerstein, G., & Brown, J. A. 1994, PASP, 106, 835
Woolley, R. v. d. R., Alexander, J. B., Mather, L., & Epps, E. 1961, R. Obs. Bull., No. 43
Woolley, R. v. d. R., et al. 1966, R. Obs. Ann., No. 2
Zinn, R. 1978, ApJ, 225, 790
———. 1985, ApJ, 293, 424